ANALYSIS OF POWER SYSTEMS WITH SELECT CYBER AND PHYSICAL CONTINGENCIES

A Thesis

by

KAUSHIK RAGHUNATH

Submitted to the Office of Graduate and Professional Studies of
Texas A&M University
in partial fulfillment of the requirements for the degree of

MASTER OF SCIENCE

Chair of Committee,	Katherine Davis
Committee Members,	Thomas Overbye
	Byung-Jun Yoon
	Astrid Layton
Head of Department,	Miroslav Begovic

May 2019

Major Subject: Electrical Engineering

ABSTRACT

The power transmission grid plays an important role in modern society and its failure has a significant impact. In the past, the grid has been subjected to malicious attack. This work focusses on maintaining the steady state stability of the grid, either under times of component failure (Such as FACT devices) or under situations of malicious attack, and then, developing techniques to analyze the system stability.

This work develops upon existing analysis techniques, such as sensitivity and clustering analysis to develop methods of mitigation of failure of FACTS devices. The analytic clustering method is compared with a Bayesian Network inference technique based technique that is introduced and developed.

Further, the mitigation technique is extended to dynamically changing operating points of FACTS devices, and the implementation for instances of failure and other states of compromised operation is discussed.

The final part presents an analysis technique, based on small signal analysis of the system to analyze the vulnerability of the system to frequency instability in instances of spoof attacks.

The results of the first part of this work explore the use of alternate techniques to improve analytic computation techniques, weighing in the benefits of the various methods, with the second and third parts addressing the impact of reactive support devices on system operation and stability, offering insights into the interaction of system parameters during steady-state and transient operation.

DEDICATION

tunbamum inbamum āgiya seivinaiyāī ulagaṅkaḻumāi * inbamil vennaragāgi iniya nal vān suvarkkaṅgaḻumāi * manpal uyirgaḻum āgip pala pala māya mayakkukkaḻāl * inpuṟum ivviḻaiyāṭṭuḍaiyānap peṟṟu ēdum allal ilanē * - śrī śaṭhakōpa, 3-10-7.

bhagavānēva svanīyāmya svarūpa-sthiti-pravritti-svaśēṣataika-rasēna anēna-ātmanā-kartrā svakīyaiḥ ca upakaraṇaiḥ svārādhanaika-prayōjanāyā paramapuruṣaḥ sarvaśēṣi śriyaḥpatiḥ svaśēṣabhūtam idam karma svasmai svaprītayē svayamēva kāritavān.

Translated: The possessor of unquantified knowledge, undiminished strength, non-eroding wealth, unsurpassed ability and energy alone, by own accord, preserver, director and propagator of all things- sentient and otherwise, with the interest on that which is countless and own, existing to adds glory, with own instruments of action, for the sole purpose of furthering the glorification of infinite unquantifiable characteristics, the distinct sentient possessor of those infinite unquantifiable honorable characteristics with none blemished who is glorified by all, known as the one along with the one who does the six tasks, upon that which adds glory, performed this action for himself and for his own accord, by himself.

ACKNOWLEDGMENTS

I thank my committee chair, Dr. Davis, and my committee members, Dr. Overbye, Dr. Yoon, and Dr. Layton, for their guidance and support throughout the course of this research. I thank all my fellow researchers at the CPMA research group for their support during my Master's program.

CONTRIBUTORS AND FUNDING SOURCES

Contributors

This work was supervised by a committee consisting of Professor Davis, Professor Overbye, and Professor Yoon of the Department of Electrical Engineering and Professor Layton of the Department of Mechanical Engineering.

The procedures discussed in Sections 1 and 2 were developed by Prof. Davis, and by Dr. Hossain-McKenzie at the University of Illinois, Urbana-Champaign between the years of 2009 and 2017. Some of the results in Section 4 were developed in collaboration with Dr. Hossain-McKenzie of Sandia National Labs in 2018.

All other work conducted for the thesis was completed by the student independently.

Funding Sources

This work was made possible in part by National Science Foundation (NSF) under Grant Number 1446471. The contents are solely the responsibility of the authors and do not necessarily represent the official views of the NSF.

NOMENCLATURE

P	Real Power
Q	Reactive Power
S	Complex Power
V	Bus Voltage Magnitude
θ	Bus Voltage Angle
G	Line Conductance
B	Line Susceptance
I	Transmission Line Current
FACTs	Flexible AC Transmission System
D-FACTs	Distributed-FACTs
SVC	Static VAR Compensator
PMU	Phasor Measurement Unit
C.I.	Coupling Index
BN	Bayesian Network
ω_s	Rated/Synchronous Speed of Generator
ω_r	Actual Speed of Generator
ARIMA	Autoregressive Integrated Moving Average
SISO	Single Input Single Output
MIMO	Multi-Input Multi-Output
DAG	Directed Acyclic Graph

TABLE OF CONTENTS

Page

LIST OF FIGURES

FIGURE Page

LIST OF TABLES

TABLE Page

1. INTRODUCTION

The power grid has seen vast leaps in operating procedures over the decades, and has, with increasing use of computer based algorithms, interoperable devices and generic procedures over the traditional use of proprietary, access restricted software, had an increasing need for cyber resilient measures. A plethora of literature exists on cyber-physical analysis of power systems, such as succeptibility of the system to cyber-attacks [1], [2] intrusion detection [3], [4], [5] and mitigation [6]; this thesis contributes towards mitigation, by analyzing the physical properties of the system.

1.1 Power System Vulnerabilities

While the primary parameters of a power transmission system, namely, V, θ, P, Q, f, cannot be directly controlled as a MIMO system, various sophisticated control techniques have emerged over the decades to maintain a standardized operating conditions for reliable power transfer. From localized control devices to regulate bus voltages to wide area power quality monitoring devices, the grid consists of multiple layers of control loops and protection devices.

Irrespective of the scale of the control loop or the nature of parameters monitored and controlled, certain elements are common to all the control loops; namely:

1. Data Generators: Sensors and State Estimators
2. Response Algorithms: Controllers and Protection Systems
3. Field Control Element

The response algorithms are designed to operate based on the parameter values that are either measured or estimated using devices and algorithms that generate a measure of the field data and condition it appropriately. Under situations of flawed data or its unavailability, the response algorithms cannot be expected to function ideally. This work focuses on such

scenarios, focusing on modifying response algorithms to suit the contingency and discusses techniques of generating contingencies that would force response algorithms to force the system towards unstable operating states.

The impact of cyber attacks on power systems can often have considerable physical impact; for instance, in 2007, it was demonstrated in [7] how cyber attacks could permanently damage a generator, utilizing relay operations. Similarly, in 2010, a Stuxnet attack [2] caused substantial damages to Iranian powerplant and in 2016, an attack on the Ukraine Power-grid caused large-scale blackouts. Given that cyber attacks have a considerable physical impact on the system, this work explores the physical properties of the system as a methods of negation and support to malicious cyber commands that modify the behavior of parts of the system. While attacks such as the latter, which involved the disconnection of substations need not be necessarily mitigated completely, the use of physical response would improve the impact of failure. It should be noted that the techniques discussed are primarily mitigative in nature, and should be used to assist system operation while appropriate techniques are used to end the cyber intrusion.

1.2 Structure of the Thesis

This work introduces existing techniques that have been developed over the past decade in Section 2, and describes the relevance and application of such techniques within the original content of this work.

Section 3 introduces a Bayesian Network based inference technique for determining the clusters of a controller online. This section details the training procedure, the inference process and the implementation for a 7 Bus system. The section concludes by summarizing the benefits, limitations of this technique viz. a viz. the existing clustering technique, and offers insights on its scope for improvement.

Section 4 focuses on the problem of failure of FACTS devices in the system (Hereafter,

interchangeably used with 'Line Controllers', 'FACTS controllers'), and, based on identifying the failed device's 'Support Group' (Defined in Section 2), devises an algorithm for recomputation of settings of other devices in the system (That need not necessarily pick up the failure). The algorithm is implemented for two cases within a 7 Bus system as proof of concept, and, the algorithm is tested for a failure scenario for the IEEE 118 Bus system. The results associated with the three scenarios are summarized in the same section.

The next two sections summarize the small signal model that is traditionally used to study the frequency stability of a system. It builds upon the classical generator model to create an optimization problem, that, when coupled with Optimal Power Flow solution techniques, would provide insights on the vulnerability of the system to a blackout, in cases of cyber-attack at its present operating point. This optimization problem accounts for buses that are deemed to be protected, and buses that are said to be 'vulnerable' to attacks. The section concludes by providing a few visualization techniques for system vulnerability and degree of freedom of system parameters.

The penultimate section summarizes the results provided in previously, and highlights the contribution of this work to existing literature. The scope for practical application of the various techniques, their limitations and potential for future research work are also summarized in the same section.

The final section provides a short conclusion of the various topics discussed in this thesis and indicates the coherence between the various topics discussed.

2. RELEVANT EXISTING TECHNIQUES

This section provides an overview of various existing techniques that are used and developed to present original ideas in later sections. This Section is divided in *3* subsections. The first subsection, §2.1 introduces the concept of coupling, it's significance in power transmission systems. §2.2 explains the process of using the computing the sensitivity matrix of a system and the use of coupling indices to study the impact of dynamic power supports (Defined for the purposes of this paper and previous literature as "controllers"). The final subsection, §2.3 explains how the techniques explained are applicable to this work.

2.1 Coupling in Power Systems

This section details the impact of coupling on system dynamics and control. *Coupling* is a phenomenon in nonlinear systems where a change in one of the *manipulated inputs* of the system results in changes in multiple *controlled outputs* of the system [8]. Power transmission systems are highly nonlinear and often, have a considerable degree of coupling of power-flows between lines. In traditional control system design, the objective would be to decouple the interaction of multiple process loops from each other.

However, within the context of power transmission systems, this is not so, for neither is the traditional definition of manipulated inputs and controlled outputs applicable, nor is coupling an unavoidable factor. Within the context of the power system, the real and reactive power demands and generations at various nodes would be treated similar to the manipulated inputs (Although, the cannot be completely manipulated) while the bus voltages, angles, line flows and system frequencies can be treated as the controlled outputs, although complete controllability of these output parameters is not currently possible. It should be noted that this segregation of parameters into manipulated and controlled variables is generalized to explain the concept, although, it is possible for bus voltages to be a

manipulated input (In the case of PV buses) etc. In such circumstances where the traditional definition of manipulated and controlled variables are not applicable and the demarcation between them is not explicit, the coupling effect of power flow in various lines is studied and in lieu of decoupling, is used to aid in system controllability, as seen in the technique developed in [9], [10].

For a power system with n buses and m lines, the coupling index (C.I.) of any two lines i and j index is defined as the cosine of the angle between the corresponding row vectors of the two lines [11]. Mathematically, it is represented as:

$$C.I.,\ cos\theta = \frac{v_1.v_2}{|v_1.v_2|} \tag{2.1}$$

Where the row vectors v_1 and v_2 are vectors containing the partial derivatives of the line power flows to the line impedance. It should be noted at this juncture that the coupling index can be defined for any two quantities in the system, so as long as a corresponding and appropriate row vector is developed. The $C.I.$ takes values in the range of [-1,1], with magnitudes closer to unity indicating stronger coupling between the lines. For the purposes of this work, the coupling sensitivities considered are that of power-flow to line impedances, although Eqn. 2.1 is applicable to sensitivity analysis using various other parameter sets.

Figure 2.1 visualizes the concept of coupling of power-flow - impedance vectors. Three vectors, two of magnitude 1.0 p.u. and one of magnitude 2.0 p.u. are represented in 3-D space. The image is sourced from [10].

The following section elucidates how the concept of coupling index is applicable and useful to power system analysis.

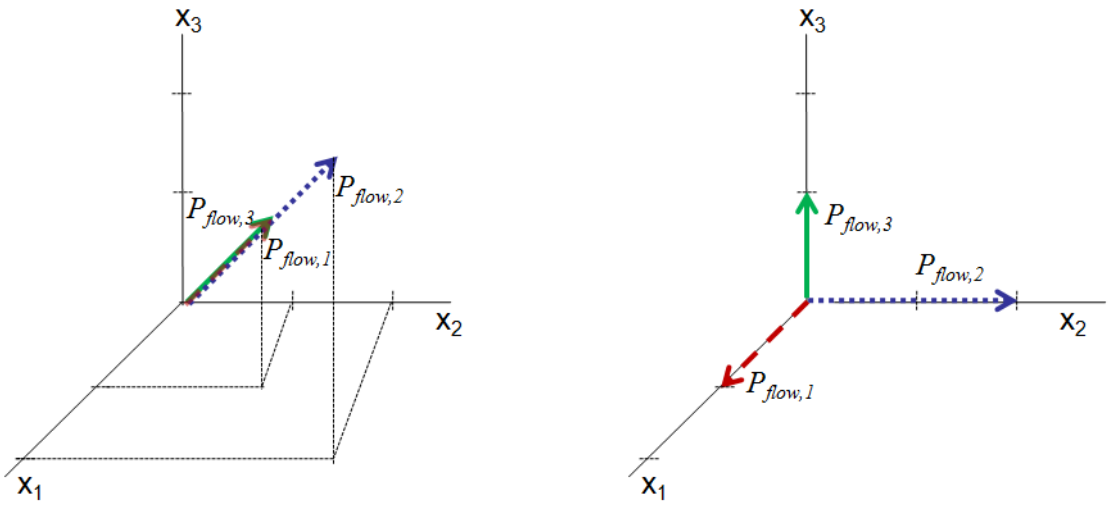

(a) Completely Coupled Lines (b) Completely Decoupled Lines

Figure 2.1: Representation of Coupled and Decoupled Power-flow vectors in impedance space of three lines.

2.2 Clustering of Lines

Clustering of lines is utilized to identify patterns in coupling of power-flows in lines and use these clusters to, on an as is required basis, to bolster system operation in instances of emergency state operation of the system.[12] and [13] define the *emergency state operation* of a system as a state of operation wherein the system is still partially or entirely functional, but, is under the verge of operating at contingency.

In order to identify potentials of support during such states of operation, the coupling index of the system is processed to further yield the sensitivity matrix and form line clusters. This (primarily) offline analysis is performed to obtain insights into the system behavior.

2.2.1 Computation of Sensitivity Matrix

The sensitivities of the power flows in system lines to change in system impedance are used in analysis that is presented in later sections of this work. Linearized sensitivity parameters between real and reactive line flows and line impedances are used to study the effects and

possible advantages of the apparent change in line impedances due to dynamic support devices on the grid.

The sensitivity equations are obtained based on the AC-PF equations of the system.

$$P_i = V_i \sum_{j=1}^{n} V_j [G_{ij} cos\theta_{ij} + B_{ij} sin\theta_{ij}] \tag{2.2}$$

$$Q_i = V_i \sum_{j=1}^{n} V_j [G_{ij} sin\theta_{ij} - B_{ij} cos\theta_{ij}] \tag{2.3}$$

Using the power-flow mismatch equations Δp_i and Δq_i ($i = 1$ to n), define a concatenated vector $f_{(p,q)}$ and vector representation of bus voltages such that

$$s_{\theta,V} = \begin{bmatrix} \theta \\ V \end{bmatrix} \tag{2.4}$$

$$\mathbf{f}_{(p,q)}(\mathbf{s}) = \begin{bmatrix} \Delta p \\ \Delta q \end{bmatrix} \tag{2.5}$$

Following this, factorizing the real and imaginary components of system impedance (i.e., conductance and susceptance respectively) into sums of partial fractions of line resistance and reactance, equations for representation of line flows can be obtained. Following this, the admittance matrix sensitivities $\frac{\partial G_{ij}}{\partial x_{ij}}$ and $\frac{\partial B_{ij}}{\partial x_{ij}}$ are computed in terms of line resistance and reactance. The array of these equations are represented using a matrix γ .

$$\gamma = \begin{array}{r} \\ nq + nv\{ \\ nq\{ \end{array} \begin{array}{c} k \\ \begin{bmatrix} \frac{\partial P}{\partial x} \\ \frac{\partial Q}{\partial x} \end{bmatrix} \end{array} \tag{2.6}$$

Where k denotes the number of lines with D-FACTS devices installed on them or will be affected directly by a FACTS device installed on a bus. These equations are used to compute

a Jacobian, J' which is defined as follows:

$$J' = \begin{array}{c} \\ np+nv\{ \\ nq\{ \end{array} \begin{array}{c} \begin{array}{cc} nq+nv & nq \end{array} \\ \begin{bmatrix} \frac{\partial \Delta p}{\partial \theta} & \frac{\partial \Delta p}{\partial V} \\ \frac{\partial \Delta q}{\partial \theta} & \frac{\partial \Delta q}{\partial V} \end{bmatrix} \end{array} \tag{2.7}$$

where nv and nq denote the number of PV and PQ buses in the system. Based on this formulation, the following relation between the concatenated mismatch vector equation, f and change in polar representation of voltages and bus angles, Δs is obtained as follows [10, p. 14]:

$$\Delta s_{(\theta,V)} = [-J']^{-1} . f_{(p,q)} \tag{2.8}$$

Based on the above definitions, a sensitivity matrix representative of the line flows to change in line admittances. Unlike the previous matrices which were sparse, this matrix, Φ is a full matrix.

$$\Phi = [-J']^{-1} . \gamma \tag{2.9}$$

Following this, the Power Flow sensitivities matrices, $Sigma$, Γ and Loss sensitivities matrix, T are defined based on the following relationships. Based on the combination of the three sensitivity matrices, the final sensitivy matrix indicative of both direct and indirect sensitivities, K is defined.

$$\Delta P_{flow} = \Sigma . \Delta s_{(\theta,V)} \tag{2.10}$$

$$\Delta P_{flow} = \Gamma . \Delta x \tag{2.11}$$

$$\Delta P_{Loss} = T . \Delta P_{flow} \tag{2.12}$$

The final sensitivity matrix, K is obtained as a measure of all the above discussed ma-

trices.

$$K = T.\left[\Sigma.\Phi + \Gamma\right] \tag{2.13}$$

2.2.2 Computation of Equivalent Line Flows

Based on the above technique, a sensitivity matrix, A'' is computed as $\Sigma.\Phi + \Gamma$ and the coupling indices is computed using its rows. The columns of A'' are decomposed using LU decomposition to identify lines in the system that can be deemed as critical, essential or redundant.

1. *Redundant Lines* are those lines which can be removed from the set of controllable lines and have no impact on overall system controllability.

2. *Essential Lines* are any minimal set of lines which together ensure complete system controllability. Essential controllers are linearly independent (Will be explained in Section 4.

3. *Critical Lines* are Essential lines that when removed from their minimal set cannot be replaced by any other line that provides complete controllability. For instance, if two sets of Essential lines $\{1, 2, 3, 4\}$ and $\{1, 2, 3, 5\}$ exist, then, controller 4 is not a critical controller. However, if no set consisting of $\{1, 2, 3, x\}$ (Where $x \neq 4$) exists, then, 4 is said to be a critical line.

Later in this work, the term *lines* will be replaced by *Controllers* as it is not useful to analyze sensitivities when no devices are available to create a change in, or, an apparent change in the line impedance.

The above classifications are identified by transforming the System Line Flow Equations (SLFE) to an Equivalent Line Flow Equation (ELFE) set, the process being as follows:

LU factorization is applied on $[A^{''}]^T$ to obtain a change of basis:

$$[A^{''}]^T = P^{-1} L_F U_b \tag{2.14}$$

$$L_F = \begin{bmatrix} L_b \\ M \end{bmatrix} \tag{2.15}$$

Using Peters-Wilkinson method [14], $[A^{''}]^T$ is decomposed (Eqn. 2.14) into its lower trapezoidal and upper triangular factors. The permutation matrix is represented using P while the triangular matrices (lower and upper) are represented using L_b and U_b respectively. M is a sparse, rectangular matrix with rows corresponding to redundant controllers. The structure of the transformed basis of $[A^{''}]^T$ is:

$$L_{CER} = {L_\beta}^T = L_F L_b^{-1} = \begin{bmatrix} I_n \\ R \end{bmatrix} \tag{2.16}$$

As in traditional controllability analysis, the new basis, (2.16), too must be full rank for a controllable system. This condition is fulfilled when $m \times (n-1)$ matrix has a column rank of $(n-1)$, where n is the number of buses in the system and m measurements of power-flow are made. L_b and U_b are nonsingular for a controllable system, and hence, rank of $[A^{''}]^T$ is obtained as the rank of the matrix ${L_F}^T$. Additionally, L_b has full rank and with (2.16) multiplied posteriorly by L_b^{-1} to the equation's RHS; thus, the row identities are preserved after the transformation ${L_F}^T$. Each row of the matrix will, therefore, correspond to the respective controllers [15].

Rows of I_n correspond to essential controls that are sufficient to assure independent controllability of the equivalent line flows. If the essential controller is the only non-zero entry of an equivalent line flow column, it is the *only* controller that can control it and is irreplaceable, that is, it becomes a critical controller. Non-zero entries in the rows of R correspond to redundant controllers while columns correspond to the equivalent flows which can easily be mapped back to the original flows using the permutation matrix P obtained from the LU decomposition step.

Now, a summary of how how the Basis Decomposition of the transposed sensitivity can be used to solve for the original linear system using back-substitution techniques is provided. The transformed basis has the following structure:

$$L_{CER} = \begin{bmatrix} I_n \\ R \end{bmatrix} \tag{2.17}$$

Where, L_{CER}, equal to L_β^T is the basis introduced in Equation (2.16). The transpose is introduced to simplify notation in the successive steps. The equivalent line flows are deconstracuted to determine the relative weightings of the actual line flows; the weightage of the elements in R (that is, their values) are examined for the redundant controllers to determine how they relate to the original sensitivities.

Considering that LU factorization is effectively Gaussian elimination. It (Gaussian elimination) is used to solve systems of linear equations by using elementary elimination matrices M_i in a sequence of steps to reduce some system matrix A into an upper triangular form. Back-substitution is then used to solve the original, linear system. Thus, using this technique in the target problem, for some linear system of the following form:

$$Ax = b \tag{2.18}$$

an elementary elimination matrix, M_1, is introduced to zero-out all elements in the first column barring that of the first row, such that only a_{11} remains as pivot. Should it initially be a zero value element, appropriate pivoting process is utilized to make it non-zero. Therefore, upon performing this operation:

$$M_1 Ax = M_1 b \tag{2.19}$$

The solution remains unchanged and the process is continued with a_{22} and successively zero

all the subdiagonal entries. This step is repeated $(n-1)$ times:

$$M_{n-1}...M_1Ax = M_{n-1}...M_1b \tag{2.20}$$

$$MAx = Mb \tag{2.21}$$

The resulting system is represented by upper triangular matrix U and solved with back-substitution. The inverse of the elementary row operation matrix is the lower triangular matrix L, and the LU factorization of (2.18) is as follows:

$$U = MA \tag{2.22}$$

$$L = M^{-1} = M_1^{-1}...M_{n-1}^{-1} = L_n...L_{n-1} \tag{2.23}$$

$$M^{-1}MAx = M^{-1}Mb \tag{2.24}$$

$$LUx = b \tag{2.25}$$

$$\therefore A = LU \tag{2.26}$$

Graphically, the above steps applied on the transposed sensitivity matrix, $\boldsymbol{L_{CER}}$, can be explained using its structure:

$$L_{CER} = \begin{array}{c} \\ C/E \\ C/E \\ C/E \\ R \\ R \\ R \end{array} \begin{array}{c} \begin{array}{cccc} Eq.1 & Eq.2 & \dots & Eq.k \end{array} \\ \begin{bmatrix} 1 & 0 & \dots & 0 \\ \vdots & \vdots & \ddots & \vdots \\ 0 & 1 & \dots & 1 \\ x & x & \dots & x \\ \vdots & \vdots & \ddots & \vdots \\ x & x & \dots & x \end{bmatrix} \end{array} \tag{2.27}$$

Where C/E/R denote Critical, Essential and Redundant controllers in the actual system equations respectively. The equivalent line flows are seen to be nothing but a linear mapping of actual line flows and that the actual system sensitivities are be obtained by traditional back-substitution solution techniques.

2.2.3 Clustering Technique

Clusters refer to a group of controllers that have similar sensitivities are are formed using the above analysis techniques. Within each group, it is only necessary to control one line flow (the target lines) because controlling one such flow impacts the others in a predictable way, reducing the control to only a few select target lines. Additionally, this technique identifies how the controllers are related to each other by finding the control support groups [16]. Given that the controllability-equivalence sets are construed through clustering using the coupling index, the selection of the number of clusters k is an important factor. Existing literature used hierarchical agglomerative clustering "as it groups data by creating a cluster tree or dendogram" [17], and is used for the results presented in later sections of this thesis.

2.3 Significance of Existing Literature to this Work

The above summarized techniques provide the basis for the results in this thesis in Section 4. A step-wise explanation of the technique, with illustrative example based on the one presented in [17] will be provided in the same section.

2.3.1 Online and Offline Application

Offline applications of the analysis technique includes identification of critical/essential lines to system operation, leveraging the sensitivities of redundant controllers to fine-tune system operation, improve controller placement and identify patterns in system operation states and states of controllers. Online applications include the usage of the technique as an optimal response process to respond to unnecessary controller settings changes, either

natural failure, unintended misoperation or adversarial presence [16] [17].

3. CLUSTERING ANALYSIS USING BAYESIAN NETWORKS

While the previous section, §2.2 summarized the use of existing clustering algorithms and sensitivity algorithms to identify support groups, this section introduces a Bayesian network (BN) approach to modeling power systems. Significant work on usage of Bayesian Networks for Power System Applications, such as Reliability calculations, State Estimation, Fault Analysis et al has been presented in [18, 19, 20, 21].

The work presented in this section builds upon existing literature, but, narrows its focus to estimating the state of dynamic reactive support devices alone. A Bayesian network is developed to represent a section of a power transmission system to predict the state of FACT controllers distributed across a power transmission system. An introduction to Bayesian network applications for power systems is provided in Section 3.1 and the rationale for using BNs for this application is explained in Section 3.2. Section 3.3 explains the methodology developed and the limitations that it may posses. The following section, Section 3.4 explains the application of the methodology and the results obtained for a small, experimental 7 Bus system. Following this, a summary of this section is provided.

3.1 Introduction to Bayesian Networks

Bayesian Networks are a type of Probabilistic Graphical Model that represents random variables as nodes and the relationship between them as edges, in the form of Directed Acyclic Graphs (DAG). Directed Acyclic Graphs are graphical models were all the edges are directed, and, no cyclic path exist in the graphical model. However, a graphical model alone is not a Bayesian Network. The DAG model combined with a Conditional Probability Distribution (CPD), with the probability of a node taking a certain value dependent on the probability of its parent nodes taking the values they have [22].

Bayesian Networks are applicable only to systems which can be expressed in the form of a Cause-Effect model, with the graph structure being reflective of the probabilistic chain

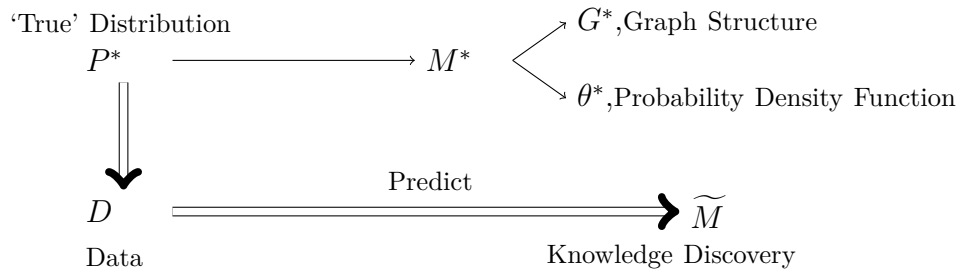

Figure 3.1: Illustration of the use of a 'True' Distribution, P^* to discover a local probability model and graph structure.

rule that is based on the given distribution of the variables.

Two important properties of BN are the local and global properties of the nodes, otherwise called Local and Global Markov assumptions. Local Markov Assumption decrees that given a node X_i and its parents, the node id independent of all its non-descendant nodes. Mathematically, $X_i \perp ND(X_i)|Pa(X_i)$. The Global Independence Property (Global Markov Assumption) states that two nodes, or, two sets of nodes are independent of each other if there exists no active trail between them. Mathematically, $(X_i \perp X_j|X_k)|d-sep(X_i, X_j|X_k)$.

Local independence properties are useful in learning of immediate neighborhood. They are used to develop global properties and develop a 'good' graph structure, where, a 'good' graph structure is said to be a graph structure that incorporates as many independence properties of the system as possible. If all the nodes in a graph are connected, then, no independence properties exist [23].

Given a distribution of data, P^*, the goal of learning techniques is to use the data to develop a local probability model θ^* and predict a graph structure, G^*. This process can be for one or more of the following objectives [24]:

1. Learn an approximate distribution of the parameters, $\widetilde{P}$ that is as close as possible to the actual distribution P^*.

2. Predictive Testing: Finding the probability of a certain set of nodes taking a certain value, given the values of the other nodes in the system. The usefulness of the developed

model for the given application can be verified using a set of validation/test data.

3. Knowledge Discovery: $\widetilde{M}$; with the goal being to infer relationships between variables. Here, a 'Confidence Score', reflective about the conclusiveness of the result is required to be estimated.

For the latter two objectives, a judicious trade-off between the variance and bias of the model is selected. A more flexible prediction, $\psi(X)$ is less sensitive and has a simpler classifier, but, is less accurate. A more accurate prediction would have a complex classifier, and also risks being over-sensitive. A lower bias allows data to be fit easier (Thus, higher flexibility), but, also has greater variance. A higher bias provides a more appropriate structure and has less variance [24].

3.2 Applicability to Context of Study

The need to activate (D-)FACTs can often be simplistic, based on a linear relationship with the current flowing through the transmission line (As seen in D-FACTS), or, at times, can be an on/off device, such as SVCs. Irrespective of the nature of the device, in scenarios of failure, the recomputation of settings of other dynamic reserve devices/controllers on-line need not be merely localized, as noted in [17].

Under scenarios where the state of the power system before failure of controller, the identity of the failed controllers is known, a properly structured BN can be used to estimate which of the remainder controllers need to be activated based on inference and simple mathematical computations, without the need to involve computation factors that process the state of the system on-line. In summary, the BNs have desirable properties for this application as they are structured based on exhaustive offline analysis to provide faster online response.

While some may opine that Neural networks can be used more effectively, under the context of this application, BNs are easier to re-train when additional controllers are incor-

porated or when the threshold for activation for a controller is reconfigured. It would be easier to retrain a BN under this context (When additional devices are added) than a Neural Network, although the latter is probably a more powerful tool. This advantage of BNs provides an avenue for it to be explored as a possible method of understand the operation of power-systems.

3.3 Training and Inference Methodology

This section elucidates on the training and inference methodology used to identify a graphical structure and determine conditional probabilities. The parameters used to generate nodes in the system were bus loads, generator dispatches, line currents and state of operation of the D-FACTs. The corresponding dataset was generated using PowerWorld for a 7-bus system under study, identical to the system studied in literature cited in previous sections.

One of the prime applications of clustering analysis is the selection of controllers to activate in the case of failure of an active controller to offset the impact of its failure. While analytical clustering analysis techniques incorporate the present operating state of D-FACTs, in the technique presented here, the operating state of D-FACTs is simplified to an ON-OFF binary, akin to most static compensators. While this may be a large generalization that removes an advantage of D-FACTs, it is done as a caution due to practical considerations, namely, generating an extremely large set of data that would result in overfitting the BN trained.

3.3.1 Training Methodology

The topological ordering is assumed using the properties of the system, such as generation is always determined based on the load demand and that the system bus voltages and line currents influence FACTs controller settings. The same properties were used to determine if a node could potentially be the parent to another node or not

A score based learning method is used to evaluate the graph structure in entirety, that

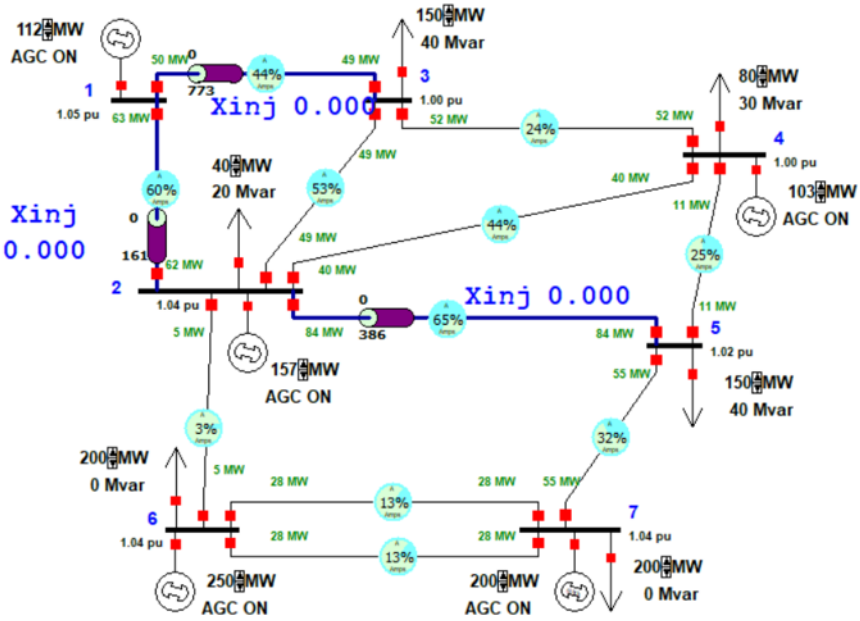

Figure 3.2: 7-Bus System used to study the usage of Bayesian Networks for System Clustering Analysis.

is, use a metric: The Goodness of a graph score, $< G, \theta_G >$ to select the most optimal graph structure. The score as a cost function that is to be maximized. The score can be obtained as a Likelihood Score or a Log Likelihood Score [25]. The Log Likelihood Score, $S_L(G, D)$ is always negative. However, this search process (for a graph structure) is simplified in this application, given that an approximate knowledge of the topological ordering of the variables is known. This provides Prior Knowledge about the Bayesian Network's structure. The Structure Score can be either of:

1. Likelihood Score– Tends to prefer more dense and near full graph structures.

2. BIC Scoring– Serves as an approximation to Bayesian Scoring.

3. Bayesian Score– Complex due to its inclusion of a structural prior. Unlike the previous

two scores, it needs to satisfy structural modularity to be decomposable, that is,

$$P(G) \propto \prod_{i=1}^{n} P(Pa(X_i) = Pa^G(X_i))$$

where $P(G)$ indicates the prior probability distribution, should be satisfied.

Since an approximate topological ordering is available and scores are inherently decomposable, the graph structure of the BN is estimated by evaluating the scores for each possible group of parents for a node. The possible combination of parent-child edges are evaluated for each individual node ('FamScore') and the combination with the highest score is selected. For any node 'i' that can assume a valid node index, the overall score of the network is defined as:

$$Score(G : D) = \sum_i (FamScore(X_i | Pa^G_{X_i} : D) - P_i) \tag{3.1}$$

A penalty term, P_i,dependent on the sum-squared distance of the prospective parent and child nodes was included to prevent the graph from getting too dense. The FamScore for each node is computed as a measure of its mutual information with the parents and its entropy. Its mathematical representation is given by:

$$FamScore_L\left(X|U : D\right) = M.\left[I_p\left(X;U\right) : D\right] \tag{3.2}$$

The mutual information of multiple nodes was computed using the following formula:

$$I\left(X;Y;Z\right) = I\left(X;Y\right) - I\left(X,Y|Z\right) \tag{3.3}$$

Based on the above formulae, each node was evaluated for the set of parents that maximized the individual FamScore for that node, that is, the set of parents that produced the least negative score was selected. Given that prior knowledge of the line coupling is known from analytic techniques covered in the previous section, after the final graph structure is ob-

tained, it is 'pruned'; wherein, excess edges are removed based on the known coupling indices between the lines. If a coupling index is approximately zero (Or, smaller than some threshold and hence, enough to be considered negligible), but, an edge is created, it is removed (or) trimmed to get the final BN.

The conditional probabilities were estimated using the data used for training and the graph structure used. Using sufficient statistics, the conditional probability is estimated as:

$$M_{\widehat{\theta}}[X_i, Pa\{X_i\}] = \frac{1}{M} \sum_{m=1}^{M} I(x_i[m] = X_i | Pa\{x_i\} = \{Pa\{X_i\}\}) \tag{3.4}$$

3.3.2 Inference Technique

The topological ordering was assumed using the properties of the system, such as generation always follows the load demand and line current determines fact controller settings. The same properties were used to determine if a node could potentially be the parent to another node or not.

3.3.3 Possible Limitations

The proposed BN's estimated parameters do not directly provide the controller settings (For non-binary controllers, such as D-FACTS), but only whether they should be computed and possibly what percentage of the maximum value the parameter can be estimated to be.

The Bayesian Network is implemented assuming that the state of the power system (That is voltage, power flows at various nodes and lines) is known while estimating whether a controller's activation is required or not. However, for practical implementation, parallel computing would be preferred to this sequential process, in which case, the system would need to be trained using fewer multinomial variables that don't need to be re-estimated, than using a larger number of binary variables.

Restraining the application to the proof of concept provided in this section, it is possible that the data generated could be insufficient to accurately model the network or that the predicted graph structure does not accurately represent the parameters.

Although they are never practically observed, a symmetric power network, should one exist would create identical data entries that will result in incorrect training and will not provide proper results. Under such cases, each individual node needs to be considered and modelled, which could result in state space explosion.

3.4 Application: 7-Bus System

The above methodology was tested on a 7-Bus/3 Controller case [26] that is serves as the demo D-FACTs case in PowerWorld Simulator. The goal is to identify a Bayesian Network structure that can be utilized to identify when a set of controllers are activated. The system parameters are converted from their multinomial range to a binomial range to generate a dataset that is used to infer the structure of the BN.

The reason for converting the multinomial distribution of power system state values to binomial models is to reduce the data size (There exists 29.3 M possible quantized combinations of system parameters using a stepsize of 0.1 p.u. for all parameters) by clustering the loads and generator dispatches into similar parameters. The semantics of the various random variables used and the threshold to quantize them as binary values are tabulated in Table 3.1.

The thresholds for declaring a parameter as 0 or 1 are selected based on knowledge of the system and observation of overload conditions. An example of the conversion is provided in Table 3.2.

The goal of training the PGM is to compute the controller settings for B_1, B_2, B_3. This is done using a few formulae if the estimate from the learned graph structure G does not

Table 3.1: Various Nodes used in the Bayesian Network. Note that there is no P_1 in the table, it contains only P_2 through P_3.

Node	Significance
I_1	Represents the current between nodes 1 and 3.
I_2	Represents the current between nodes 1 and 2.
I_3	Represents the current between nodes 2 and 5.
B_1	Represents the status of the controller of line between nodes 1 and 3.
B_2	Represents the status of the controller of line between nodes 2 and 3.
B_3	Represents the status of the controller of line between nodes 2 and 53.
P_2	Real power at node 2. Takes additional subscript of G/L depending on whether it indicates generation or load.
P_3	Real power at node 3. Takes additional subscript of G/L depending on whether it indicates generation or load.
P_4	Real power at node 4. Takes additional subscript of G/L depending on whether it indicates generation or load.
P_5	Real power at node 5. Takes additional subscript of G/L depending on whether it indicates generation or load.
P_{Gen1}	Real power generation at node 1.
P_{Gen2}	Real power generation at node 2.
P_{Gen4}	Real power generation at node 4.

Table 3.2: Converting a multinomial distribution into a binomial distribution.

Parameter	P_{L2} (p.u.)	P_{L3} (p.u.)	P_{L4} (p.u.)	P_{L5} (p.u.)	G_1 (p.u.)	G_2 (p.u.)	G_4 (p.u.)	I_1	I_2	I_3	B_1	B_2	B_3
Actual States	0.4	0.4	0.4	0.2	0.2	0.55	0.8	49%	31%	54%	0	0	0
Binomial Conversion	0	0	0	0	0	1	1	0	0	1	0	0	0

imply that the controller should be Off (That is, zero). One of the advantages of doing so is to avoid the computation of matrix inverses. The Assumed Topological Ordering is: P_2,P_3,P_4,P_5 followed by P_Gen1, P_Gen2, P_Gen4, I_1, I_2, I_3 followed by B_1, B_2, B_3.

While computing using matrices, for a specified P_2 through P_5, the rest of the parameters are calculated, that is, generation and system parameters depend on the load demand. This is treated as non-mathematical prior knowledge and hence, they are listed first, as they cannot have parent nodes. However, after that point, it is difficult to ascertain distinctly which parameters affect which others, yet, given that the generalized sequence is to determine bus voltages then compute dispatches, both of which affect bus currents and hence, line currents, a pattern of Generator Dispatches followed by Line Currents and finally D-FACTs state is chosen. While it would be intuitive to state that only generation affects the line currents, certain combinations of parameters simulated on PowerWorld Simulator shows that it is possible for the line current to decrease when certain bus' load profile and another bus' generation increase, due to the nonlinear nature of the network. Hence, the line currents are evaluated with both load and generation as possible parents.

The Dataset generated using PowerWorld Simulator has 503 observations (Akin to the example illustrated in Table 3.2), with 439 observations used to train the BN. 64 observations were used to validate the BN.

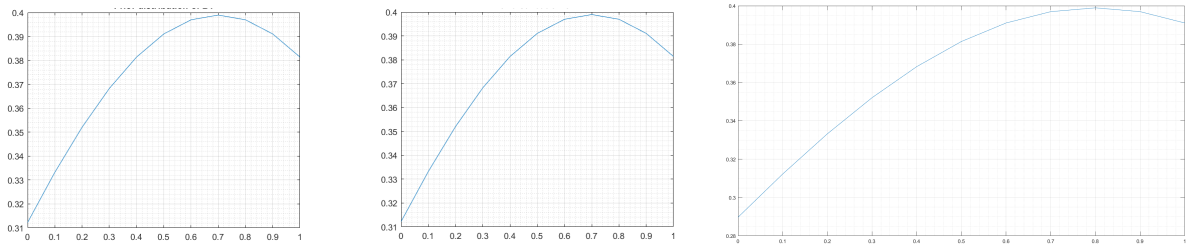

(a) Assumed normal prior for Controller 1. (b) Assumed normal prior for Controller 2. (c) Assumed normal prior for Controller 31.

Figure 3.3: Normal Prior Curves assumed for the 3 Controller nodes.

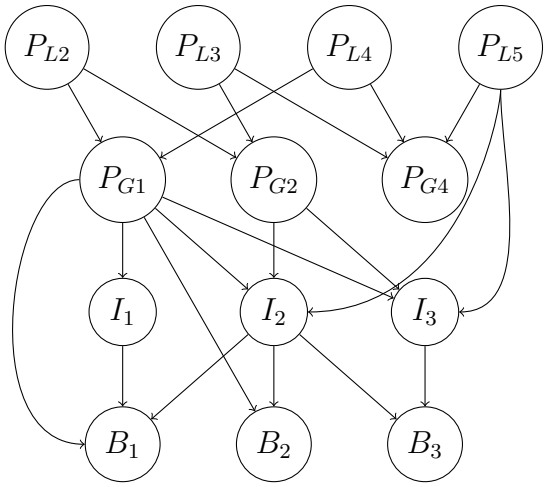

Figure 3.4: Initial Bayesian Network Graph Structure

Based on the analytic system analysis, it was noted that the edge between I_2 to B_3 exists in the BN, although its coupling index is approximately zero. Hence, this edge is pruned to get the final BN, shown in Fig. 3.5.

3.5 Results and Summary

The validation was done by generating observations for power, voltage and current nodes and estimating the probability of B_1, B_2, B_3 being unity. 64 Observations that were unused in the training of the network were used to validate the graph. These datasets were used to check for True Positives, True Negatives, False Positives and False Negatives.

The nine tabulations (In the appendix) list the conditional probabilities that were estimated based on Fig 3.5. Based on the conditional properties, it is observed that the correlation between load demands and generation is either linear or an exponential relation. However, there is no strictly increasing or decreasing trend between the line currents and controller states with their respective parents. All the priors assumed were normal distribution curves with peaks at 0.7, 0.7 and 0.8 for B_1, B_2, B_3 respectively. The priors assumed a variance of unity, and depending on the location of the peaks of the posterior, controllers were either set to on or off states.

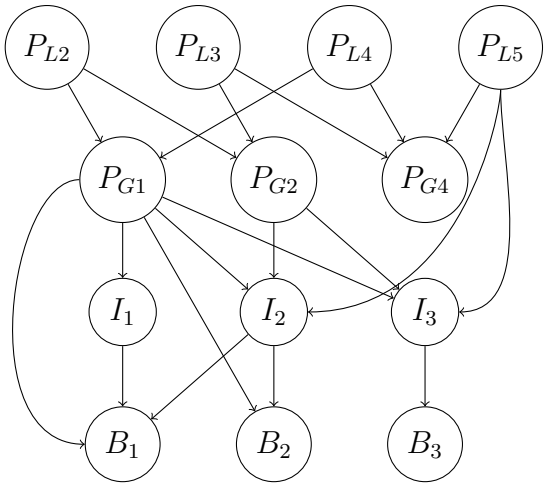

Figure 3.5: Pruned Bayesian Network Graph Structure, with edge between I_2 and B_3 removed.

Table 3.3: Validation results for Controller # 1, B_1

	No. of occurrences	% of Results
True Positive	35	54.688%
True Negative	26	40.625%
False Positive	0	0%
False Negative	5	4.687%

Based on the above priors, the results of the 64 tabulations (Simulated Vs Graphically predicted) are shown below. The definitions of True Positives/Negatives et al. are as follows:

1. True Positive: Both the simulation and the predicted structure predict B_x=1.

2. True Negative: Both the simulation and the predicted structure predict B_x=0.

3. False Positive: The graph structure predicts B_x=0 while the simulation predicts B_x=1.

4. False Negative: The graph structure predicts B_x=1 while the simulation predicts B_x=0.

In real life cases, false positives would not cause system instability, only increase the cost of operation, and possibly force certain local response systems to act. However, false negatives, which could cause a key controller to not turn on, could cause line overloads or

Table 3.4: Validation results for Controller # 2, B_2

	No. of occurrences	% of Results
True Positive	14	21.875%
True Negative	26	40.625%
False Positive	12	18.75%
False Negative	12	18.75%

Table 3.5: Validation results for Controller # 3, B_3

	No. of occurrences	% of Results
True Positive	26	40.625%
True Negative	20	31.25%
False Positive	8	12.5%
False Negative	10	15.625%

not provide crucial reactive support. The following image (Fig. 3.6) graphically illustrates the percentage of true predictions for each controller, with B_1 corresponding to the highest number of predictions. It could be due to the reason that B_1 was activated more often than the others, followed by B_3 and then B_2.

If one neglects the economics of operation, assumes that an unnecessary operation of a D-FACTs device does not necessarily cause system instability, and group the True predictions and False Positives as acceptable results, the results improve, with the probabilities of taking an incorrect action being 0%, 18.75% and 12.5% respectively. While this is not an acceptable rate of inaccuracy, supplementing the activation logic with various other measurements and operator knowledge could help improve the results.

The predicted Bayesian Network had over 95% accuracy while predicting the state of Controller 1, with poor results for the other two controllers. When the economics of operation of operation were factored out, the 'accuracy' of controller 3 improved to 87.5%, while controller 2 did not see a considerable leap in its prediction. The prediction accuracy can most probably be improved when the other elements in the power system (Bus voltages and phase angles, lines without controllers installed) are factored into the graph. It is

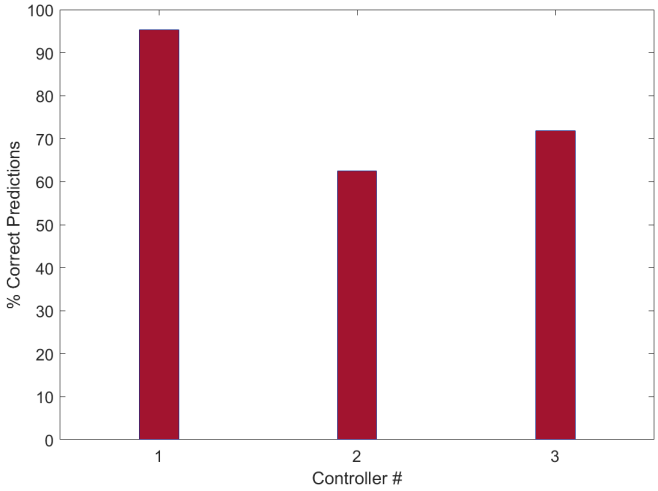

Figure 3.6: Graphical illustration of the Percentage of the correct predictions (TP + TN) for the three controllers.

hypothesized that inclusion of other line currents (that is, lines with no direct connection to D-FACTs) could improve the results for controller 2. Results of controller 3 could be improved when a relationship between it and other controllers is considered and factored into the structure inference step.

4. DISTRIBUTED FACTS FAILURE MITIGATION*

This section provides insights into the recomputation techniques used in system recovery technique during distributed controllers' failure, based on the methods developed in Chapaters 2.2 and 3. This section focuses on the methodology of recomputation of settings of controllers in support groups. The role of this methodology within the overall framework of controller failure response (Such as the ones discussed in [17]), is highlighted by the green box in Fig 4.1 (Base Image: [27]).

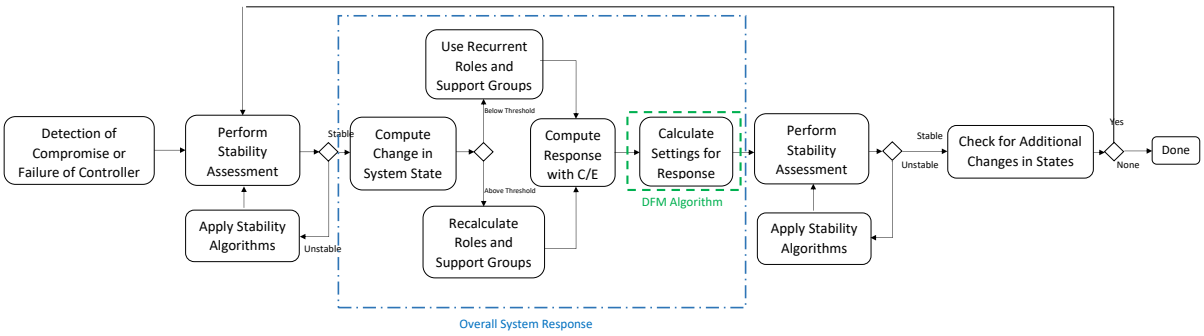

Figure 4.1: Mitigation of Distributed Controller Failure, highlighting the role of the DFM algorithm and the overall system response.

This section is organized as follows: Section 4.1 provides an overview of the solution technique, followed by Section 4.2, which explains the mathematical models developed and employed in the technique. Section 4.3 introduces and elucidates on the Distributed Controller Failure Mitigation (DFM) Algorithm. The following sections, 4.4 and 4.5 provide results of the application of this technique to a 7-Bus system and the *IEEE* 118-Bus system.

*Parts of the results presented in this section are reprinted with due acknowledgments from 'K. Raghunath, K. Davis, "Mitigation of Distributed Controller Failure", Clemson Power Conference, Sep 2018', with the reprinted material indicated as per copyright holder (IEEE) requirements.

The final section summarizes and concludes this section.

4.1 Overview of DFM Algorithm

The use of Flexible AC Transmission (FACTS) devices on transmission lines provide a technique of controlling power flow between buses while improving the cost-effectiveness and reliability of the grid's operation. The DFM Algorithm is a technique of computing the settings of any variable FACTS device, with multiple devices on the same line or bus modeled in bulk. The algorithm proposes a technique for mitigation of the effect of a dysfunctional controller ('Dysfunctional' and 'failure' is defined for the purposes of this thesis as FACTs that do not operate at the desired settings) through analysis of the effect of other controllers in the system on the concerned line to determining corrective actions in the settings of the other devices, while accounting for stable range of bus voltages and angles of the system.

The primary motivation for developing such mitigation techniques is to compensate for controller failure in system operations. For instance, a failure of a FACT device would result in an increase in line current, which could be picked up by a protective relay. While monitoring need not necessarily result in the tripping of breakers, it is an undesired event.

The DFM algorithm computes the maximum corrective action that can be made by other FACT devices in the system through online computations. The selection of the other FACT devices for effective mitigation can be done via online or offline analysis techniques, such as the ones discussed in [17]. A reference list of effective controllers that can compensate for the failure of the controller in focus is created and used as rlookup in the algorithm to make corrective computations. The computations determine the change in the effective line impedance that is required from the compensating controllers to mitigate the failure. Based on the type of FACT device, the p.u. change in impedance can be converted to a proportional control signal that triggers the device to make the corresponding reactive injections

into the line.

This algorithm assumes that the failure of the device and its location is known, and based on prior knowledge of the coupling effect of other controllers on the dysfunctional controller's line, the algorithm selects a set of functional controllers and performs computations based on the proposed algorithm to compensate for the increase in line current due to the controller failure. For example, in order to determine a device's failure, periodic estimation of the line impedance using the reactive power flowing through the line and comparing the estimated value with the results of the line impedance estimated using the operating state of the controller can be used as a technique for detection.

4.2 Mathematical Models Used

The DFM algorithm uses previously available data of load and generation distribution and knowledge of controller support groups (Explained in literature review) to perform online computations to find the new settings of the devices. The selection of controller support groups can be done via offline analysis, as seen in *Recurrent* techniques that are discussed in [17], or, using online techniques. The results presented later in this section use offline analysis, that is, *Recurrent* techniques. Details on the selection techniques are presented at the end of this section where they are brought up for discussion.

DFM computes change in effective line impedance(s) required using the AC Power Flow equations and Newton-Raphson iterative method to solve them. For some bus 'i'. the real and reactive power consumed are expressed using the equations:

$$P_i = P_{Gi} - P_{Li} = |V_i| \sum_{j=1,\neq i}^{n} |V_j|(G_{ij}cos\theta ij + B_{ij}sin\theta ij) \tag{4.1}$$

$$Q_i = Q_{Gi} - Q_{Li} = |V_i| \sum_{j=1,\neq i}^{n} |V_j|(G_{ij}sin\theta ij - B_{ij}cos\theta ij) \tag{4.2}$$

Table 4.1: Tabulation of parameters used in the DFM algorithm.

n	Number of buses
m	Number of lines
M	Number of controllers modeled in bulk (In the case of D-FACTs, M $\leq$ m)
c	Number of controllers that have failed
z	Number of controllers in the identified support group
V_i	Voltage at bus 'i'
θ_i	Voltage angle at bus 'i'
S_i=P_i + jQ_i	Complex power at bus 'i'
S_{Gi}=P_{Gi} + jQ_{Gi}	Complex power injection at bus 'i'
S_{Li}=P_{Li} + jQ_{Li}	Complex power consumption at bus 'i'
Y_{Bus} = G +jB	Admittance matrix of the system
Subscripts	
i,j	Bus indices (0 $\leq$ i, j $\leq$ n)

Since conductance of lines (G) is usually far smaller than its susceptance (B), G is ignored. Additionally, it should be noted that since the results of this algorithm are susceptive quantities computed by using partial derivatives, even a significant value of conductance does not considerably affect the final results; however, there is a small negligible effect, due to the nature of the system reactance being affected by dynamic support devices. Thus, upon this simplification, the equations are reduced to De-Coupled line flow equations, as follows:

$$P_i = P_{Gi} - P_{Li} \ = |V_i| \sum_{j=1,\neq i}^{n} |V_j|(B_{ij} sin\theta ij) \tag{4.3}$$

$$Q_i = Q_{Gi} - Q_{Li} \ = |V_i| \sum_{j=1,\neq i}^{n} |V_j|(-B_{ij} cos\theta ij) \tag{4.4}$$

The above equations are differentiated partially with reference to the line susceptance for all target lines, that is, lines with FACTS devices. For some line l_{ij} (j = 1 to n, j $\neq$ i), the partial derivatives of the power flows with respect to that line's susceptance is used. These

derivatives are reflective of the direct sensitivity elements of the sensitivity matrix described in the §2.1.

$$\frac{\partial P_i}{\partial B_{ij}} = |V_i||V_j|sin\theta_{ij} \tag{4.5}$$

$$\frac{\partial Q_i}{\partial B_{ij}} = |V_i||V_j|cos\theta_{ij} \tag{4.6}$$

In an ideal condition where all bus voltage magnitudes are 1.0 p.u. and bus angles zero degrees, the partial derivatives of real power tend to zero and the partial derivatives of reactive power tend to unity. While this is not practically feasible, these ideal conditions serve as a equality constraint that can be implemented in the DFM algorithm as a internal constraint during iterations for correction computations. These conditions are flexible, and can be replaced with any other constraint that is deemed necessary, depending on the scenario.

$$\frac{\partial P_i}{\partial B_{ij}} = |V_i||V_j|sin\theta_{ij} \ = 0 \tag{4.7}$$

$$\frac{\partial Q_i}{\partial B_{ij}} = |V_i||V_j|cos\theta_{ij} \ = 1 \tag{4.8}$$

Using the above two equations of the partial derivatives of real and reactive power with respect to line susceptance, which play the role of an internal checker for the algorithm's computations during iterations, the DFM algorithm computes the change in susceptance of the target device. A convention of first utilizing partial derivatives of reactive power, before real power, is chosen so that the matrix formed as a result of the above computations is not singular. A matrix consisting of only the partial derivatives of reactive power, or the partial derivatives of reactive power and real power, will have elements that are both (approximately) unity and zero, thus not being singular. A highly impractical scenario of interconnecting all buses with each other would cause the matrix formed to be a singular

matrix. Since it is highly impractical, the matrix formed is considered to be always invertible. One corrective computation (That is, a non-iterative computation scheme) is made for each coupled controller based on the clustering results. For a system with 'n' buses, 'm' lines, 'M' controllers (M $\leq$ m) and 'c' failed controllers, computations are performed using less than 'm – c' partial derivative equations and can use a minimum of 'm – M + c' partial derivative equations for validation. A controller with strong coupling to all other controllers would require the maximum number of computations, that is, (m – c) computations. The usage of equations is summarized in Table 4.2.

Table 4.2: Summary of Partial Derivative Equations Utilized in the DFM Algorithm.

Equations Available	Control Computations Required	Equations Available for Validation
2m	$\leq$ m - c	$\geq$ m - M + c

4.3 DFM Algorithm Methodology

The detection of controller failure can be performed using estimation techniques and one of the possible estimation techniques has been briefly states in Section I. Assuming that the dysfunctional controller has been detected, the DFM technique operates using the following steps:

1. Identify location of controller(s) under failure or misoperation.

2. Check if any limits or constraints have been violated. If they have not and the correction is deemed unnecessary, exit algorithm.

3. Form a mathematical construct where the devices are operating at their default/zero state settings. If it is a misoperation and not a failure, substitute the default value with the available estimate of operating point.

4. Look up controller support groups to form a Support Susceptance Group column vector, B' containing the effective susceptance of lines affected by devices in the support group.

5. If any of the devices in the support groups have failure, eliminate them from Support Susceptance Group column vector.

6. Eliminate multiple listing of controllers in B'.

7. Assign 'z' = Size of B'.

8. If any voltage and bus phases violate any constraints and have not been addressed by a local response device, set them to the pre-failure value in the computation constraint.

9. Compute $\frac{\partial Q_{ij}}{\partial B_{ij}} \forall\, i = 1...n, i \neq j$

10. If $z > m$, compute $\frac{\partial P_{ij}}{\partial B_{ij}} \forall i = 1...z - m, i \neq j$

11. Form Susceptance Jacobian matrix, J_s of magnitude $'z \times z'$ based on the partial derivatives.

12. Form function vector, $F_s = [Q_1 Q_2 ...]^T$ of row length 'z'.

13. Compute $\Delta B = -J_s^{-1} F_s$

14. Use ΔB to update the base Y_{Bus} matrix and convert the apparent change in susceptances to controller settings.

15. Verify that voltage and bus angle limits are not violated by using a fast approximation technique.

16. If required, hone the controller settings using further iterations.

17. Stop

Once the devices are detected, the DFM algorithm is designed to respond only if necessary. The algorithm illustrated above highlights one of the possible scenarios in which it is designed to execute. The rationale for this is straightforward; it is to prevent unnecessary computations in scenarios where local response devices are sufficient to address the undesired state of operation, or, in scenarios where the effect of failure in negligible on system operation state. Once the algorithm is triggered, a column vector consisting of the default settings of the devices in the case of failure, or, in the case of the last known operating state of the device if it misoperates and is at a different setting. This column vector is defined as B_x, with the elements being the effective line susceptance in the case of D-FACTs.

$$B_x = [B_{fl1} B_{fl2} B_{fl3} ...]^T \tag{4.9}$$

Once the devices under failure or misoperation are identified and the need to utilze the algorithm is determined, they are mapped to their Support Group Clusters to obtain the set of devices that can be used to mitigate the effect of failure or misoperation. Depending on how the support devices are selection, the following selection techniques are utilized [17].

1. *Recurrent CE Selection*: Recurrent CE selection techniques are support group selection schemes that utilize the history of the system's operating states to choose support controller selection. Thus, Recurrent Selection techniques are useful in offline analysis, allowing for support groups to be looked up. Recurrent CE Selection Technique utilizes a history of the power system states and clustering analysis across the states to form clusters of system devices that play a critical or essential role to system controllability.

2. *Recurrent R Selection*: Computed in the same technique as described above, it is a selection technique that selects devices that have a redundant role in enforcing system controllability.

3. *Current CE Selection*: Current Selection techniques utilize the present operating point of the power system and can be utilized as an online tool. The *Current CE Selection*

performs equivalent line flow analysis of the system when a failure is detected and then selects the most effective Critical and Essential Controllers that can be utilized.

4. *Current R Selection*: Similar to the Current CE Selection, the *Current R Selection* performs online analysis to utilize redundant controllers for system response.

5. *Ranked R Selection*: Similar to other redundant selection techniques, the *Ranked R Selection* utilizes redundant controllers, but, utilizes them in a ranked order of their impact on coupling.

Selection techniques that utilize Critical and Essential devices are always more effective in mitigating device failure and misoperation than redundant devices. However, redundant devices can be utilized to provide additional changes in settings that can assist moving the system closer to its original state under scenarios where the settings of Critical and Essential devices are saturated and additional 'thrust' in the direction of saturation is required.

In scenarios where a support device is unavailable, either because its settings are saturated, or, if it too is not properly operational, then, it can either be replaced in the B' vector by its redundant counterparts, or, if no redundant counterparts exist, it is eliminated from the vector and the remaining devices are utilized for mitigation. At times, it is possible to have a controller multiply listed in B' (When two devices in the same support group fail simultaneously) and hence, before computations are performed based on it, it is filtered for redundancies/multiple listings.

The power system computation is set up utilizing that last available system state estimation, with any violations and changes set to the state during the last available system state estimate during non-failure. This can include voltages, bus angles (directly) and power-flows on transmission lines (indirectly). The direct constraints can be set as voltage and bus angle set points. Power-flows can be incorporated as additional inequality constraints, or, be converted to an equivalent voltage-bus angle combination that mathematically yields the desired power-flow and enforce those values as an equality constraint.

The above details are considered to be data pre-process for the core of the algorithm. Steps 1 – 8 of the algorithm correspond to this; the core of the DFM algorithm Newton-Raphson method to compute the change in susceptance that is required by supportive controllers to enforce the desired system constraints (Demonstrated in results with system voltage and bus angles within tolerable limits). Since complete control of system cannot be achieved with the failure of a critical controller, the DFM algorithm does not make multiple iterations to re-compute a possible combination of controller settings that will best satisfy a set of constraints and limits. In such cases, a solution that would satisfy a majority of convergence criterions are selected as the final results.

The matrix J' is used as a Jacobian to compute the change in line susceptances that is required. It is formed using equations partial derivatives; and is employed in a manner similar to the Jacobian matrix formed for power flow calculations to estimate the bus voltages. However, the derivatives used in the latter are with respect to bus angle and voltage, while the proposed method uses derivatives with respect to susceptance. Based on the computed value of J', the calculated vectors are substituted in the formula for multivariable Newton-Raphson iterative solution and the change in solution is calculated. This is then updated to get a new B_x. The corresponding equation is expressed below.

$$B_x^{i+1} = B_x^i - J'^{-1} F_s \tag{4.10}$$

For scenarios where multiple iterations of corrective computations are implemented, the convergence criterion for the algorithm is set to satisfy both the following three relationships. Although there is no explicit constraint on the bus angles, they are implicitly accounted for in the second constraint. Any other additional constraints can be added on to these three. These three only form a minimal set of convergence criterion, and are not an absolute representation on the constraints under which the DFM algorithm can operate.

$$|V_i - 1.0| \leq \epsilon_v \, \forall \, i = 1, 2...n \tag{4.11}$$

$$|\frac{\partial P_i}{\partial B_{ij}}| \leq \epsilon_P \, \forall \, (i,j) \tag{4.12}$$

$$l_{flow(i,j)} \leq l^{lim}_{flow(i,j)} \, \forall \, (i,j) \tag{4.13}$$

Where parameter ϵ is a small convergence criterion close to zero. Additionally, the tolerance limit for voltage ϵ_v can be varied based on known operating history, system PV characteristics, or a desired set point, in the case of PV buses. A summarized illustration of the above process is depicted in the flowchart in Fig. 4.2.

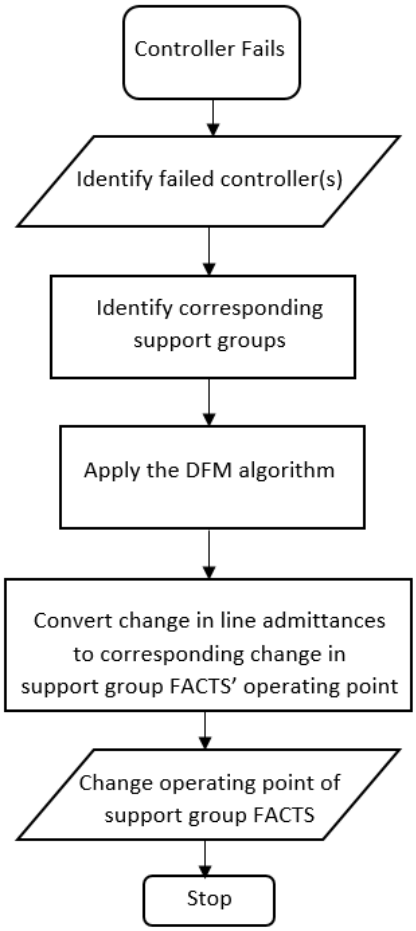

Figure 4.2: Simplified Flowchart depicting a summary of the steps performed in the DFM algorithm.

4.4 Application: 7-Bus System

The application of the DFM algorithm is divided into two parts. The first of the parts concentrate on utilizing the DFM algorithm to recompute D-FACTs settings while the second focuses on the role of the algorithm in larger system response. The role of the two parts discussed in these results in overall system response is presented in Fig. 4.1. The computation of equivalent line flows in overall system response, based on existing literature is highlighted in the first subsection below. The 7-Bus system is depicted in Fig. 4.3.

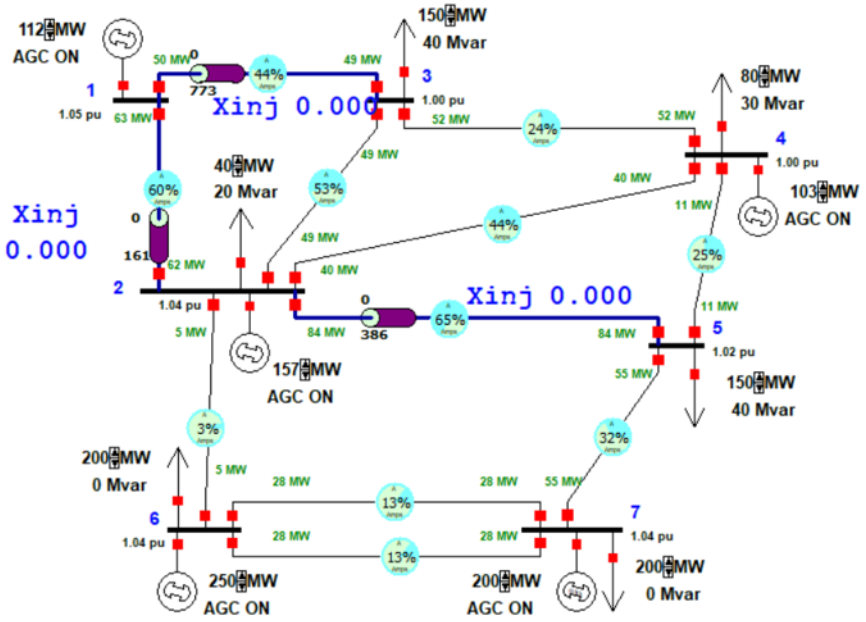

Figure 4.3: 7-Bus System used to illustrate DFM Algorithm and Overall Algorithm

4.4.1 Equivalent Line Flows

This section demonstrates the computation of equivalent line flows for the 7-bus system operating at a load distribution (In per unit) of [1.12 1.57 1.50 0.80 1.50 3.0 2.0]. It should be noted that parts of the results presented below are published in [17]. The D-FACTS scenarios demonstrated in this scenario utilize the sensitivity of total power flow (In MVA)

to line impedance, based on the AC power flow equations. The sensitivities are computed analytically, reflecting both direct (i.e., change in impedance of a line and its direct impact on that line's power flow) and indirect (i.e., change in impedance of a line and its indirect impact on all other lines' power flows) sensitivities [10].

While the results presented in this section of the thesis discus mitigation strategies of a power system using D-FACTS, the methodology developed is independent of the type of device and can be extended suitably to any dynamic control support to the power grid. While methods presented in this paper are generic and can be used for any power system, due to the nonlinear nature of power systems, it is possible that controllers installed on certain lines cannot mitigated using the support group responses developed. This could be due to two causes, either that the support groups cannot sufficiently manipulate the power flow in the line of the controller under concern or that no support groups exist. Such circumstances can be averted by optimal controller placement and including redundancies.

The *line flow groups* are discovered by cluster processing of the sensitivity matrix's rows. The Cosine similarity of row vectors $\mathbf{v_i}$ and $\mathbf{v_j}$ of $\mathbf{A}''$ (coupling index) is used to find coupled sets of lines as clusters that are approximately orthogonal to each other [28]. Following this, the set of *critical*, *essential*, and *redundant* controllers are calculated by decomposing the transposed sensitivity matrix using LU decomposition. The *critical*, *essential*, or *redundant* status of a controller is determined based on the coupling of the columns of $\mathbf{A}''$ (rows of $[\mathbf{A}'']^{\mathbf{T}}$). Applying LU factorization to $[\mathbf{A}'']^{\mathbf{T}}$ yields a change of basis, decomposing it into two triangular matrices [14]. The equivalent numerical structure of the Upper Triangle of the decomposed Sensitivity matrix can be found in Table 4.3 (Originally published in [27]).

Utilizing the decomposed basis's inverse, the transformed basis of the form below (in equation 4.14) is obtained. The value of the matrix elements in the given (above) operation

Table 4.3: Representation Upper Factor matrix of the Sensitivity Matrix for 7-bus system. The corresponding results are presented in Table 4.12.

	T1	**T2**	**T3**	**T4**	**T5**	**T6**
EQ.L1	1.9165	-0.3014	0.6138	0.4783	-0.7696	1.3766
EQ.L2	0	-1.6761	-0.5473	-0.7116	-0.9459	0.4046
EQ.L3	0	0	-1.4221	0.7592	-0.7507	-0.6497
EQ.L4	0	0	0	1.2547	-1.2407	1.2444
EQ.L5	0	0	0	0	-0.0041	0.0113
EQ.L6	0	0	0	0	0	-0.0063

state is represented in table 4.4.

$$\mathbf{L_{CER}} = \mathbf{L_\beta}^{\mathbf{T}} = \mathbf{L_F L_b^{-1}} = \begin{bmatrix} \mathbf{I_n} \\ \mathbf{R} \end{bmatrix} \tag{4.14}$$

Table 4.4: Representation of Transformed Basis matrix, L_{CER} for 7-bus system. The corresponding results are presented in Table 4.12.

	EQ.L1	**EQ.L2**	**EQ.L3**	**EQ.L4**	**EQ.L5**	**EQ.L6**
I_n	1.0	0	0	0	0	0
	0	1.0	0	0	0	0
	0	0	1.0	0	0	0
	0	0	0	1.0	0	0
	0	0	0	0	1.0	0
	0	0	0	0	0	1.0
C_R	-0.0015	0	0	0.090	0	0
	-0.0145	0	0	0.923	0	0
	0	1.51	0	-0.002	-1.064	0.746
	-0.125	0	0	-0.187	0	0

Writing the results of Table 4.3 in the form of equations:

$$\mathbf{EQ.L1} = 1.9165 \cdot T_1 - 0.3014 \cdot T_2 + 0.6138 \cdot T_3 + \tag{4.15}$$
$$0.4783 \cdot T_4 - 0.7696 \cdot T_5 + 1.3766 \cdot T_6$$

$$\mathbf{EQ.L2} = -1.6761 \cdot T_2 - 0.5473 \cdot T_3 - 0.7116 \cdot T_4 \tag{4.16}$$
$$- 0.9459 \cdot T_5 + 0.4046 \cdot T_6$$

$$\mathbf{EQ.L3} = -1.4221 \cdot T_3 + 0.7592 \cdot T_4 - 0.7507 \cdot T_5 \tag{4.17}$$
$$- 0.6497 \cdot T_6 \tag{4.18}$$

$$\mathbf{EQ.L4} = 1.2547 \cdot T_4 - 1.2407 \cdot T_5 + 1.2444 \cdot T_6 \tag{4.19}$$

$$\mathbf{EQ.L5} = -0.0041 \cdot T_5 + 0.0113 \cdot T_6 \tag{4.20}$$

$$\mathbf{EQ.L6} = -0.0063 \cdot T_6 \tag{4.21}$$

The above equations (4.15) - (4.21) are the linear mapping between the target line flows and the equivalent line flows that can be seen in Table 4.3. The corresponding ranking of redundant controllers can be seen in Table 4.5.

The transformed basis indicates the ranking of redundant controllers; they are primarily designed to operate when compromise or failure occurs for any essential controllers (in their corresponding column in $\mathbf{I_n}$). The entries of $\mathbf{R}$ give the sensitivity of each equivalent line flow to each redundant controller. For example: If the essential controller of **EQ.L4** is compromised, from the transformed basis it is clear that redundant controller C_{R2} has the highest impact on **EQ.L4**. C_{R4} has the next highest sensitivity and is followed by C_{R2}. Both C_{R1} and C_{R3} have low sensitivities and would not be effective if used alone. Essential controllers with no redundant controller support have corresponding entries of 0 in R. Based on the specific compromise or failure situation, these rankings can be used to employ the most sensitive redundant controllers or utilize all controllers such that highly ranked controllers

are prioritized. Table 4.5 summarizes the ranking of the redundant controllers for the six equivalent line flows computed for a selected operating point of the system.

Table 4.5: Ranking of Controller groups in descending order of the effectiveness using equivalent line flows for the 7 Bus system.

Ranking of Redundant Controllers		
Equivalent Line	**Effective Controllers**	**Ineffective Controllers**
EQ.L1	$C_{R4} > C_{R3} > C_{R2}$	C_{R3}
EQ.L2	C_{R3}	C_{R1}, C_{R2}, C_{R4}
EQ.L3	N/A	C_{R1}, C_{R2}, C_{R3}, C_{R4}
EQ.L4	$C_{R2} > C_{R4} > C_{R1} > C_{R3}$	N/A
EQ.L5	C_{R3}	C_{R1}, C_{R2}, C_{R4}
EQ.L6	C_{R3}	C_{R1}, C_{R2}, C_{R4}

While the above results are sufficient for *Current* selection techniques, they are insufficient for *Recurrent* selection techniques. In order to cluster the lines and obtain support groups, the 7-bus system's operating states are studied with upto variations of $\pm 30\%$ of the line impedance, which is based on the practical device limits [26] [17]. With these operating points and device combinations, controller role and control support groups are recalculated and compared. Using this process on multiple devices to generate a large set of operating points, patterns of *recurrent essential controllers* and *recurrent critical controllers* are discerned. Controllers $1, 2, 3, 8, 9$ frequently appear as essential. The numerical results of these analysis is identical to original work developed in existing literature [27]; hence, it is not included here.

Based on the above analysis, the overall system response to controller failure is decided.

4.4.2 Results: DFM Algorithm Tuned Settings

The DFM algorithm was tested for a few controllers in the system under two conditions-scenarios where the algorithm in not required and scenarios where the algorithm is required. Both scenarios were considered to verify the security and dependability of the algorithm's

operation respectively. Results are initially presented for one iteration of computation, and then for multiple iterations. The *effectiveness* metric utilized in the results is the deviation from 1.0 p.u. voltage magnitude.

In the following results, originally published in [29], it is seen that the chosen criterion of bus voltages being closer to an ideal value do not improve with multiple iterations of the DFM algorithm. Thus, it can be concluded that it can be used non-iteratively for small systems to provide effective mitigation. This conclusion is illustrated as a plot of bus voltages for the 11 controller system; there exists a relatively greater difference in bus voltages between iterations (when compared to the 3 controller case). However, on absolute terms within the scenarios themselves, the difference is negligible.

The first set of results are presented for the PowerWorld Demo case of the 7-Bus system [26], that has three D-FACTs installed. The 7-bus system is divided into 3 areas with 11 transmission lines, 2 of which run parallel from bus 6 to 7. Although there are no FACT Devices installed on the lines, the algorithm would consider the equivalent effective impedance by both lines in computations. In such a case (As described in section VII), the overall susceptance change required by the lines is computed by the algorithm and another topology sensitive algorithm needs to be added to obtain the individual changes required.

The present case has D-FACTs installed in lines 1-2, 1-3 and 2-5. The devices are current sensitive, active when line current is between 75% and 100% of rated limit. They vary the effective admittance of the lines up to 30% of the base value, which correspond to $j5.94$, $j1.2413$ and $j2.4827$ respectively. The algorithm is applied to a situation in which the controller from bus 2 – bus 5 fails. The algorithm is tested for two conditions:

1. The controller fails, but at a juncture where no injection is required.
2. The controller is in operation, but becomes dysfunctional suddenly, that is, injects 0.0 pu of susceptance.

Since the voltages in the base test case are close to unity, a sum squared error is computed considering the bus voltage magnitudes and ignoring the angles. It is computed as follows:

$$E = \frac{\sum_{i=1}^{n} (V_i - V_{sp})^2}{n} \tag{4.22}$$

The initial results presented are computed with a single iteration of Newton-Raphson solution. The 'limits' referred to in the tables are the maximum change in line susceptance that can be achieved by a D-FACTs device. In situations where the computed correction value is greater than the maximum achievable limit, the correction value is set to the achievable limit.

The 'suggested ΔB' parameters in the tables is the change in line susceptance that is required to compensate for the failure of controller(s) under scrutiny, post-saturation. This is a generic quantity that can be used to compute the new settings of a FACTs device based on its operation principle. While all results herein are indicative of D-FACTS, these parameters can be used to compute the settings of any generic FACTs device by converting the values of ΔB to change in line impedance and computing the operating point of the device that would cause such a change in the line impedance. In the case of controllable shunt devices connected to buses, two or more lines are incorporated into the algorithm reflective of that device, and once the results are obtained, suitable computations are performed to convert the change in susceptance to the change in firing rate of the device.

Although controllers on all lines are impractical and superfluous, this case is considered as it contrasts the fundamental scenario seen above, where there are more equations for validation than the ones required for computation. This condition requires the maximum number of corrective actions (Up to 10) to be computed and offers the minimal number of equations (3) to validate the model.

In the case of failure at non-zero injection condition, it is observed that the required change in operating points of the other controllers in the same cluster group exceeds the

maximum possible change in operating point of the controller. For both these two test scenarios with the same system topology, the DFM algorithm suggests a change in the operating points of the other controllers even when the controller in concern does no inject any reactance into the line. In results that correspond to condition 1 (p. 45), the results should be indicative of a zero magnitude change, but, a minor change was noticed. This is a result of two successive stages of approximation involved at estimating the bus voltages and the limitations in the number of iterations used.

Tables 4.6 through 4.11 illustrate the effect of iterations on the currently chosen *effectiveness* metric, namely, maximum deviation of bus voltage from nominal voltage. It is seen that there is no significant gain (for the selected system and its operating point) obtained by using multiple iterations.

The first tabulated result presented is for the 7-Bus, 3 Controller case (Table 4.6) where controller between buses 2-5 is in operation, but, the algorithm is still tested to compute new settings for the other two controllers in the system. It is observed that there is a minor change computed by the algorithm even in this scenario. The reasons for this have been summarized previously in this section.

Table 4.6: Testing the security of DFM Algorithm on 7-Bus, 3 Controller case using the controller on line between buses 2-5. Computed using one iteration of DFM algorithm. © IEEE, 2018.

Computed ΔB_{12}	Computed ΔB_{13}	E
j0.0093	-j0.03	0.0015

Following this, the DFM algorithm is tested on the same system for a scenario where the controller on line between buses 2-5 is operational. The system load distribution for this result remains the same distribution of [1.12 1.57 1.50 0.80 1.50 3.0 2.0] p.u., for which the above equivalent flows were elucidated. The results are presented in Table 4.7.

However, the above result goes beyond the possible changes in line impedances that

Table 4.7: Testing the dependability of DFM Algorithm on 7-Bus, 3 Controller case using the controller on line between buses 2-5. Computed using one iteration of DFM algorithm. © IEEE, 2018.

Computed ΔB_{12}	Computed ΔB_{13}	E
j0.1677	-j0.124	0.0025

can be obtained by operation of D-FACTs. Thus, following the saturation of the D-FACTs settings at the maximum possible value ($\pm 30\%$), the results obtained as as follows, surmised in Table 4.8.

Table 4.8: Testing the dependability of DFM Algorithm on 7-Bus, 3 Controller case using the controller on line between buses 2-5 and considering D-FACTs setting limits. Computed using one iteration of DFM algorithm. © IEEE, 2018.

Computed ΔB_{12}	Computed ΔB_{13}	E
j0.0168	-j0.0459	0.003

Following the demonstration of results for the PowerWorld Demo case with 7-buses/3 Controllers, a set of results for the 7-buses/11 controllers case is demonstrated. The operating state remains the same, and the results correspond to the stepwise computation of equivalent power-flows detailed in the previous section.

Table 4.9: Testing the dependability of DFM Algorithm on 7-Bus/11 Controller case using the controller on line between buses 2-5 and considering D-FACTs setting limits. Computed using one iteration of DFM algorithm. © IEEE, 2018.

Computed ΔB_{12}	Computed ΔB_{23}	Computed ΔB_{34}	Computed ΔB_{45}	E
j0.0459	j0.0604	-j0.2412	-j0.0805	0.024

Following the above preliminary results that were obtained using single iteration computations, the DFM algorithm is executed for algorithms for the results corresponding to

Tables 4.8 and 4.9. The corresponding *effectiveness* metrics are presented in tables 4.10 and 4.11. Following a short remark on the results, discussion on these results are presented at the end of this section, after discussing the overall system response.

Table 4.10: Variation of *Effectiveness* Metric with increase in iterations of DFM Algorithm for 7-Bus, 3 Controller case in Table 4.8.

Scenario	Maximum ΔV	E
Failure State	0.05	-
Single Iteration	0.0252	0.0021
Three Iterations	0.0252	0.0021

Table 4.11: Variation of *Effectiveness* Metric with increase in iterations of DFM Algorithm for 7-bus/11 Controller case in Table 4.8.

Scenario	Maximum ΔV	E
Failure State	0.05	-
Single Iteration	0.0232	0.024
Three Iterations	0.0253	0.022

It is observed that in the case of the 7-bus/11 Controller case that although the *effectiveness* metric improves with increase in iterations, the maximum deviation of a bus voltage from ideal per unit value (Set to be unity for all buses in this case) also increases. It is also observed that the bus voltages do not improve with multiple iterations of the DFM algorithm and can be said that, for small systems, single iteration is sufficient to be effective.

4.4.3 Results: Overall System Response

The controller settings are computed using the DFM algorithm illustrated above. The first result presented is indicative of the settings used to demonstrate the overall algorithm, while the second demonstrates a more practical application; the usefulness of the algorithm

in relieving loaded lines, under a different load profile. The 7-Bus system is illustrated in 4.3.

For Controller #2 (compromised) with a high flow, the overall system response is demonstrated for a *Recurrent CE* group comprising of controllers $\#1, 2, 3, 8, 9$. The response does not make any assumptions on the control objective developed either as a result of misoperation, or, adversial intrusion in operation. The Recurrent CE selection algorithm is most successful in reducing the line flow, where the loading of Line 2 is reduced from 55% MVA to 48.9% MVA.

Table 4.12: Responding to Controller 2 Compromise with Various Response Controllers (C#) and Settings; Original $\text{MVA}_{L2} = 44$ %. Reproduced from [27].

Controller #2 Compromise ($x_{DF} = -0.072pu, 55\%$ MVA$_{L2}$)			
Selection Method	**Response C#**	**New x_{DF} (pu)**	**MVA$_{L2}$**
Recurrent CE	1,3,8,9	-0.015,-0.054,0.072,-0.018	48.9%
Recurrent R	4,5,6,7,10	-0.054,-0.036,0.018,-0.009,-0.072	51.4%
Current CE	4,5,7,8,9	-0.054,-0.036,-0.009,0.072,-0.018	51.1%
Current R	1,3,6,10	-0.015,-0.054,0.0171,-0.072	49.3%
Current Ranked R	1,10	-0.015,0.072	53.4%

In a second scenario (demonstrated below), again with controller # 2, The *effectiveness* metric is changed in the last scenario to demonstrate that the overall response algorithm can be implemented for different control objectives, with the key to efficacious results being implementation of appropriate selection methods. The *Recurrent CE* selection algorithm is found to be the most effective in this scenario while the ranked R is found to be the least effective.

Following these initial results that include manual explained steps, the overall response is demonstrated for a much larger system, in the following section.

Table 4.13: Responding to Controller 2 compromise with various response controllers (C#) at high load in the 7-bus system; Original $MVA_{L2} = 89$ %. Mean line flow is used as a metric as the original system (before compromise) was structured to have similar line flows on all other lines.

Controller #2 Compromise (Original Line Flow: 89% MVA_{L2})			
Selection Method	**Response C #**	**MVA_{L2}**	**Mean of all other line flows MVA_{L2}**
Recurrent CE	1,3,8,9	79.6%	53.0%
Recurrent R	4,5,6,7,10	71.1%	56.4%
Current CE	4,5,6,7	76.7%	55.4%
Current R	1,3,7,10	76.6%	58.2%
Current Ranked R	1,3,10	79.9%	56.1%

4.5 Application: 118-Bus System

The IEEE 118-Bus system (Fig. 4.4) is tested for a single controller failure and a coordinated controller attack. In first case demonsrated using this system, the controller on line 63 (illustrated in orange in Fig 4.4) is selected as the compromised controller, with Controllers # 50, 68, 69 and 117 selected using the *Recurrent R* method, acting as the support groups, highlighted in blue in Fig 4.4.

It is observed that the failure of the controller on Line 63 increases the overall real power transmission loss by 4.03% and reactive power transmission loss by 57.71%. After the recalculation of settings of the other controllers, the real power transmission loss did not improve, while the reactive power transmission loss improved by 11% over the failure state. These results are presented in Table 4.15. Additionally, Fig 4.5 visualizes the transmission losses for the three scenarios (Before and during compromise of controller, Post mitigation) as a fraction of the overall load demand of the system.

It was observed that post mitigation, a minor increase (of 0.87 MW) in real power transmission losses existed, but, a considerable decrease in reactive power losses. This pattern is observed across all such mitigations, and can be observed in the later results presented in this section (Table 4.17). The recomputation of the settings of the other devices provides a notable decrease in reactive power loss.

Following the above scenario of failure of a single D-FACTs device, the overall response

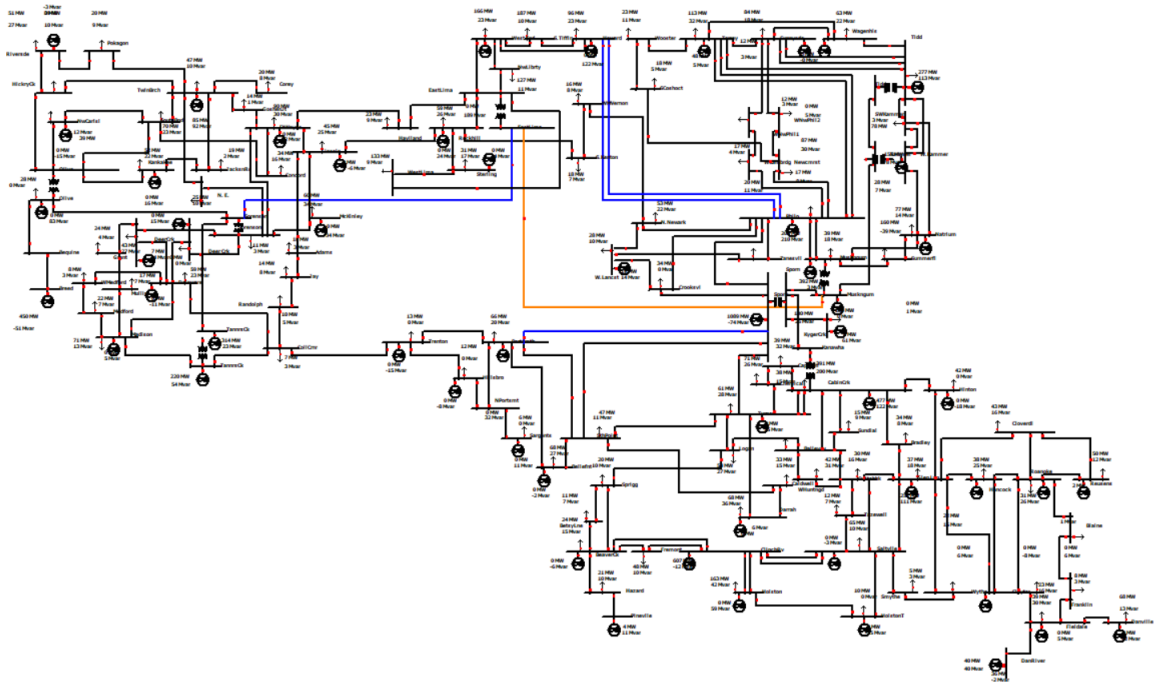

Figure 4.4: IEEE 118-Bus system used to demonstrate overall system response. The orange line is indicative of the single D-FACTs device under failure while the blue lines indicate the response controllers.

strategy is demonstrated for a scenario of coordinated attack, where several essential controllers on Lines 14, 63, 81 and 117 are compromised. The aim of this attack is to reduce power-flow on lines with high capacity and force it to be routed through lines with low capacity. The SDCD recomputes settings of controllers in other high capacity lines to mitigate this event. In this scenario, the high capacity lines have functional D-FACTS devices that enable higher power-flow. Considering a scenario where these devices are compromised, which leads to an increase in the effective impedance of these lines and forcing power to reroute through other lines, increasing the loading on those lines that reduces the overall system efficiency, and, at certain instances, cause a line to almost be fully loaded. In this scenario, other controllers in the concerned support groups are selected and reconfigured with the objective of rerouting power-flow through these support lines to improve system efficiency while reducing the loading on lines that witnessed an increase in flow through

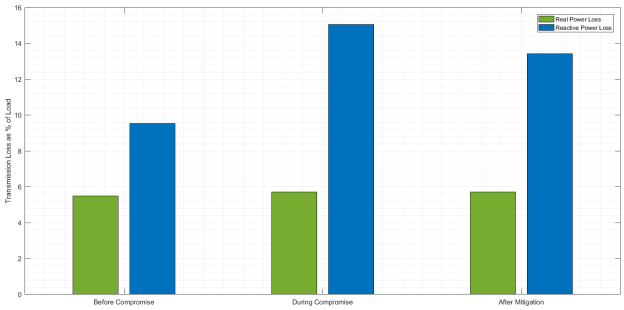

Figure 4.5: Summary of the Transmission Losses in the 118-Bus system before and during the compromise of a controller, and post mitigation of failure, highlighting the considerable increase in reactive power loss and negligible increase in real power loss.

Table 4.14: Summary of the % MVA flows in the target lines during failure and post-correction for the IEEE 118-bus system with the objective to reduce target line's flow.

Controller #63 Compromise (Original: 84.76% **MVA$_{L63}$)**		
Line #	**% MVA During Failure**	**% MVA Post-Correction**
63	94.76%	84.6%
50	21.55%	28.32%
68	36.75%	41.25%
69	36.75%	41.25%
117	63.58%	75.71%

them. Table 4.16 provides a summary of the MVA flows in the lines during the functional state of the target essential controllers during a coordinated attack. Table 4.17 provides data pertaining to overall system efficiency that indicates how SDCD strategy can be used to move the system closer to its original operational state during times of an attack, with the metric of system losses being used here. In this juncture, it is pertinent to note that the selection algorithm used for not the most effectively performing one, but, one of lower effectiveness. It is pertinent to note from the results that the overall response is effective even in scenarios where *only* controllers with lower impact (*Recurrent R* selection), that is, redundantly ranked devices, are available for mitigation. Using more effective techniques such as *Current CE, Recurrent CE* etc. will provide more benefit. The results of these other selection techniques are compared in Table 4.17.

Table 4.15: Summary of the real and reactive power flow losses in the IEEE 118-bus system for a single controller attack scenario with the objective to reduce target line's flow.

Controller #63 Compromise (Original: 84.76% **MVA$_{L63}$)**				
Scenario	**Real Power Loss (MW)**	**Reactive Power Loss (MVAr)**	**% Increase in Real Power Loss**	**% Increase in Reactive Power Loss**
Before Failure	257.87	137.11	N/A	N/A
During Failure	268.08	216.54	4.03%	57.713%
Post Correction	268.25	192.84	4.09%	40.6%

In summary, the IEEE 18-Bus system was tested for scenario of compromise and recalculation of settings of other controllers provided a satisfactory reduction in the power-flow in the target line (that was compromised) and showed a distinct improvement in the overall system efficiency.

Table 4.16: Change in line flows for a coordinated attack on essential controllers 14, 63, 18 and 118 using Recurrent R selection technique.

S. No	Line Number	Controller Role	Power-Flow in Line (MVA)		
			Before Attack	During Attack	After Mitigation using Recurrent R selected controllers
1	14	Essential (Under Attack)	89	85	86
2	19	Mitigative	10	10	10
3	50	Mitigative	100	103	106
4	63	Essential (Under Attack)	400	388	385
5	68	Mitigative Parallel Lines	162	166	174
6	69		162	166	174
7	81	Essential (Under Attack)	36	33	32
8	93	Mitigative	39	40	43
9	117	Essential (Under Attack)	171	162	158
10	118	Mitigative	134	140	149

4.6 Summary and Conclusion

The proposed algorithm to recompute settings provides an effective and considerable corrective action to meet a control objective (Such as, compute settings while a voltage

Table 4.17: Comparison of the effectiveness of selection techniques for the 118-Bus system. It is observed that considerable improvement in losses are obtained even with redundant (less effective) controllers.

S. No	Mitigation Selection Technique	Losses
-	Normal Operation	264.471 MW, 181.327 MVAR
-	Coordinated Attack Scenario	268.076 MW, 216.541 MVAR
1	Recurrent R	268.024 MW, 202.711 MVAR
2	Recurrent CE	268.917 MW, 187.337 MVAR
3	Current Ranked R	266.258 MW, 200.315 MVAR

range is not violated) and in situations of failure of non-critical controllers, the algorithm provides corrective results that can offset the effect of failure.

The matrix inversion computed in the algorithm is not impractical for all practical configurations except the case all buses are connected to all other buses. Since such a scenario is extremely improbable, it is concluded that the DFM algorithm is not restricted by system topology. The selected matrix is sparse, hence, suitable matrix inversion techniques can be applied to make the computations feasible for larger systems.

The proposed methodology offers insights into designing operating ranges of controllers to obtain better compensation in situations of failure, computing the support a controller is expected to provide, and replacing it with the maximum value possible if the ceiling is exceeded. However, for cases where there exists no coupling effect of adjacent lines on a transmission line, this algorithm cannot be implemented.

The results of the change in *effectiveness* metric in the results of the 7-Bus system provides certain key insights into the system operation. While the *Current CE* and *Current R* techniques (that factor-in the present operating point) provide a better reduction of power-flow in Line 2 (the compromised line), when the measure of effectiveness is changed, selection techniques that depend primarily on the system topology perform better. These results indicate that the SDCD algorithm's flexibility is effective in both restoring a system's overall

line flows to the original state before a compromise, or, restoring that of a particular line alone. Depending on the objective, an appropriate selection technique can be used.

The results for the single controller attack scenario in the 118-Bus system provide multiple key insights into the results: i) The results reiterate observations from the 7-bus system that the line clusters and support groups need not be necessarily localized, and they are highly dependent on system topology as well as the distribution of loads and generators across the system; and, ii) results indicate how to utilize knowledge of the system to generate remedial schemes that ensure grid operation without limit violations using distributed controllers in the system rather than merely using localized elements/devices in the immediate neighborhood. It should be noted at this juncture that within the context of the selected contingency, *larger parts* refers to lines a couple of nodes away and not lines that are connected to (electrically) far away nodes.

In conclusion, the DFM algorithm provides an effective technique of recomputing the settings of devices that, as a part of a larger response process that achieves mitigation of failure and/or misoperation of distributed dynamic support devices to meet a desired control objective.

4.7 Comparison of Bayesian Network and Analytic Clustering Techniques

The analytic clustering techniques provide various selection techniques such as *Recurrent R, Current R* etc., allowing the flexibility of choosing an appropriate technique that suits the control objective. On the other hand, The Bayesian Network trained scheme provides neither of these selection techniques, but rather, a mix of both. While the selection of devices is primarily based on the current operating point of the system (Corresponding to *Current* selection techniques), it is highly influenced by the total history of system that was used to generate the Bayesian Network, which corresponds to the *Recurrent* selection techniques.

The Analytic clustering techniques allow the choice to either selection C/E controllers or Redundant devices. This cannot be directly implemented in the BN based method.

One simple and expensive solution is to generate datasets corresponding to each selection technique and train a BN for each. However, given that this involves massive amounts of redundancies, a simpler solution is to identify the states of all C/E controllers in the BN and infer only the states of the redundant devices.

Another solution would be to use a combination of the two techniques, using the analytic techniques to compute the support groups while the Bayesian Network takes the place of the DFM algorithm, providing the new settings. While the demonstrated example uses binary states and hence, cannot be compared directly to the DFM algorithm, better quantization of (D-)FACTs settings while training the Bayesian Network would allow it to be interchangeably used with the DFM algorithm.

5. POWER SYSTEM VULNERABILITY ANALYSIS

This section introduces power system vulnerability analysis using the transient small signal frequency stability model. The presence of system parameters in the stability equations is leveraged to build a mathematical model of the system that can be used for both developing system attacks as well as develop mitigation strategies. This section starts by introducing state space modeling of a system in Section 5.1 and the following section, Section 5.2 provides an introduction to the small signal stability model of a power system that has been traditionally used and explains why it is used despite better transient models being available. The mathematical model developed is explained in the succeeding section and the applications of the model are summarized afterwards. The application of the model to a few small systems are explained and the finally, comprehensive results for the IEEE-118 Bus system are presented at the end. Following this, an explanation of how the model developed can be utilized as a defense technique against itself are explained, followed by a few applications that are explained conceptually.

5.1 State Space Modeling

State Space Modeling of a system is a representation of the system variables in terms of a mathematical construct relating 'internal states' with system inputs and outputs. The internal states of a system, often labeled as 'x', is defined as the minimal set of variables pertaining to the system that can completely represent the system at some given instant of time. The system input variables, u, and output variables, y are represented as a construct of themselves and the internal states. Mathematically,

$$\dot{x} = Ax + Bu \tag{5.1}$$

$$y = Cx + Du \tag{5.2}$$

In the above equation pair (State Equation and Output Equation), the parameter vectors utilized are (i) Controlled Inputs (u), (ii) System States (x), and (iii) System Outputs (y). The matrices utilized are:

1. 'A' = State transmission matrix, capturing the relationship between the state variables and the rate of change of state variables.

2. 'B' = Input matrix, depicting the relationship between the input vectors and state variables.

3. 'C' = Output matrix, depicting the relation between the internal states and the output variables.

4. 'D' = Feedforward matrix (Usually zero matrix).

It can be seen from the fact that the D matrix is usually zero that the internal states of the system play a critical role in system model, and hence, must be selected such such that there are minimum uncertainties in its estimate/measurement. The state variables perform four functions [30], namely:

1. Memory: The state variables capture an effective summary of the history of the system.

2. Internal variables that along with their derivatives can be used to represent any output variable.

3. Minimality: Since the number of state variables selected are a minimal set, no further simplifications are possible without compromising the order of the equations being order 1 (linear).

4. Non-Uniqueness: "Any set of n-independent internal variables, not directlyconnected to the input, represents the system. By independent we meaneach one representing a different storage process." (Quoted from [30, p. 23]).

State Space modeling is a powerful tool that can be applied for both SISO and MIMO systems, given that it places no initial condition constraints (such as zero initial condition of Laplace transforms).

Stability of a system represented by State Space Modeling is checked using the State Transmission Matrix. Stability is checked using eigenvalues of State transmission matrix; mathematically, this can be proved by converting state space to transfer functions:

$$\frac{y(s)}{u(s)} = C(sI - A)^{-1}B + D \tag{5.3}$$

This is also reflected practically. For instance, Controllability is defined as a measure of the ability of the controlled input to force a state of the system from one value to another in finite time. Although this classical definition intuitively indicates that only the B matrix plays a role, it not so. Transition from one state to another depends on both present state and input. For example: Different magnetic fields are produced in an electromechanical device depending on whether it is saturated or not, even when you increase the input voltage by the same amount. Mathematically too, controllability matrix is computed using both A and B matrices, by checking the rank of a compound matrix formed by the adjunct matrix formed by the products of the A and B matrices [31, 30].

Figure 5.1 represents the State Space representation of a system, highlight the variables and equations.

However, despite all these powerful benefits, State space modeling needs adaptation for usage in power systems. The points of conflict are

1. No system I/Os in Power Systems that match the traditional definition of controlled inputs and system outputs.

2. The availability of excess variables: What is the criterion for categorizing a parameter as a state, input or output variable?

3. What parts of the system and what variables should be considered to make it to one

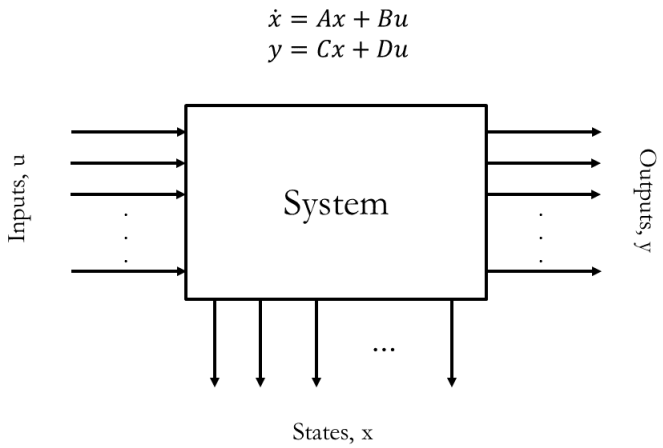

Figure 5.1: State Space Representation of a system.

of the three categories?

4. State space modeling is for linear systems. Power Systems are not linear, how can they be adapted suitably?

5. What power system model do you use for modeling? Different models for different scales (Steady state PF models, transient models).

While the traditional definition of controlled inputs and outputs are not directly applicable in this context, existing literature has utilized linearized power system equations (AC-PF) to represent them in the form of state space models, with transient models being invariably represented as linearized state space equations, with the linearization being performed around the system operating point [32]. The selection of the input, state and output variables is dependent on the model, and, one such model that is utilized is explained in the following section.

5.2 Power System Small Signal Stability Analysis

The Small Signal Model of a Power System is a Transient Time representation of the system frequency based on the parameters of the generation and transmission system [33]. It utilizes the [mechanical] radial speed of the devices connected electrically to the system, the

grid electric frequency, machine inertial constant, internal machine voltages and equivalent line impedances. It is a fundamental model, simplifying many of the system behaviors. It assumes that the mechanical power input to the [rotational] generator, P_m, is constant, that the damping of the machine is negligible, that the voltage behind the transient reactance is constant (Fig. 5.2) and that the rotor angle and voltage angle are in phase not only during steady-state operation, but, also during transient operation [33].

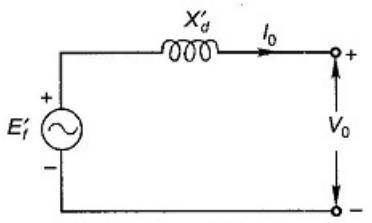

Figure 5.2: Transient Circuit Representation of Synchronous Generator with internal and terminal voltages, transient reactance labeled that is used in iterative calculations.

While more accurate and sophisticated models exist, the Small Signal model is utilized for the analysis as it provides a simple mathematical construct that can be used to optimize a selected objective based a cost function derived from the mathematical construct. The parameters utilized are explained in Table 5.1.

For some bus 'i' ($1 \leq$ i le n_g), the power angle, δ_i at that bus is defined as:

$$\delta_i = \omega_i - \omega_s \tag{5.4}$$

The rotor radial speed is represented as a function of the system's electric and mechanical parameters:

$$\omega_i = \frac{\omega_s}{2H_i}\left[P_{m,i} - E_i G_{ii} - \sum_{\forall j \neq i}^{n_g} E_i E_j (B_{ij} sin\delta_{ij} + G_{ij} cos\delta_{ij})\right] \tag{5.5}$$

The equation of radial speed is nonlinear, and hence, cannot be represented as a state space system of the form $\dot{x} = Ax + Bu$ and $y = Cx + Du$. Thus, the two equations are

Table 5.1: Tabulation of parameters used Power System Small Signal Frequency Analysis.

n	Number of buses
n_g	Number of buses with generators
m	Number of lines
V_i	Voltage at bus 'i'
θ_i	Voltage angle at bus 'i'
ω_i	Machine radial speed at bus 'i'
ω_s	Machine mechanical radial frequency at bus 'i' that corresponds to grid electrical radial frequency.
S_i=P_i + jQ_i	Complex power at bus 'i'
S_{Gi}=P_{Gi} + jQ_{Gi}	Complex power injection at bus 'i'
S_{Li}=P_{Li} + jQ_{Li}	Complex power consumption at bus 'i'
Y_{Bus} = G +jB	Equivalent Admittance matrix of the system of order n_gxn_g
Subscripts	
i,j	Bus indices ($0 \leq$ i, j $\leq n_g$)

linearized around the operating point of the system. Let $\delta^* = [\delta_1\ \delta_2...\delta_{n_g}]$ represent the operating point vector of the equivalent system (With non-generating nodes equivalenced) at all buses. The corresponding radial frequency set-point would be $\omega^* = [\omega_{s1}\ \omega_{s2}...\omega_{sn_g}]$.

Based on this linearization, the system state variables (x) are assigned as change in power angle, $\Delta\delta_i$ and change in radial speed, $\Delta\omega_i$. However, the power angle requires a reference, and thus, $\Delta\delta_1$ is selected as a reference, and the remaining power angles are converted to changes in angles, $\Delta\theta_i$. Thus, the state variables are:

1. $\Delta\theta_i$ (i = 2 to n_g)

2. $\Delta\omega_i$ (i = 1 to n_g)

The state vector is formed in the form $x = [\Delta\omega_1\ \Delta\theta_2\ \Delta\omega_2\ \Delta\theta_3...]$. The corresponding equations used to compute the A matrix are:

$$\frac{d}{dt}\Delta\omega_i = \frac{\omega_s}{2H_i}\left[-\sum_{\forall j\neq i}^{ng} E_i E_j \Delta\delta_{ij}(B_{ij}sin\delta_{ij} + G_{ij}cos\delta_{ij}\right] \tag{5.6}$$

$$\frac{d}{dt}\Delta\theta_k = \Delta\omega_k - \Delta\omega_1 \tag{5.7}$$

where the indices i, k range from 1 to n_g and 2 to n_g respectively. Once the corresponding A matrix is computed, its eigenvalues are computed to check for system stability. If all the eigenvalues have real parts that do not life in the Right Hand Side Plane of the Real-Imaginary plane, the system is stable.

5.3 Mathematical Analysis

This section provides the usage of the State Transmission Matrix, A, explained in the previous section to develop a mathematical model that can be used to optimize for a set of system parameter values that are used in the applications illustrated later in this section.

The State Transmission Matrix computed has elements that are either zero, unity (± 1) or some functional value dependent on the system state. The form of the matrix is:

$$A = \begin{bmatrix} 0 & \neq 0 & 0 & \neq 0 & 0 & \cdots & \neq 0 & 0 \\ -1 & 0 & 1 & 0 & 0 & \cdots & 0 & 0 \\ 0 & \neq 0 & 0 & \neq 0 & 0 & \cdots & \neq 0 & 0 \\ -1 & 0 & 0 & 0 & 1 & \cdots & 0 & 0 \\ \vdots & \vdots & \vdots & \vdots & \vdots & \ddots & \vdots & \vdots \\ -1 & 0 & 0 & 0 & 0 & \cdots & 0 & 1 \\ 0 & \neq 0 & 0 & \neq 0 & 0 & \cdots & \neq 0 & 0 \end{bmatrix} \tag{5.8}$$

The elements of -1 and $+1$ correspond to $\Delta\theta_k$ parameters, derived from $\Delta\omega_k - \Delta\omega_1$. The nonzero values indicated correspond to element values of $\Delta\omega_i$, reflecting the system parameters and operating points. There are patterns in the A matrix, but, they cannot be leveraged unless the terms are regrouped to collect all the zero and unity elements together.

In order to leverage the matrix's patterns, the state variables are reordered as:

$$x = \begin{bmatrix} \Delta\theta_2 \\ \vdots \\ \Delta\theta_{n_g} \\ \Delta\omega_1 \\ \vdots \\ \Delta\omega_{n_g} \end{bmatrix} \tag{5.9}$$

By grouping all the angle and speed terms together, a broad pattern emerges in the A matrix. It can be divided into five smaller sections, two sections of zero matrices, a section with an Identity matrix, a column vectors of all elements -1 and a matrix of order n_gxn_g reflective the system parameter and states. The resultant matrix is of the form:

$$A = \begin{bmatrix} 0 & \cdots & 0 & -1 & 1 & 0 & \cdots & 0 \\ 0 & \cdots & 0 & -1 & 0 & 1 & \cdots & 0 \\ \vdots & \ddots & \vdots & \vdots & 0 & \vdots & \ddots & \vdots \\ 0 & \cdots & 0 & -1 & 0 & 0 & \cdots & 1 \\ \neq 0 & \cdots & \neq 0 & 0 & 0 & 0 & \cdots & 0 \\ \neq 0 & \cdots & \neq 0 & 0 & 0 & 0 & \cdots & 0 \\ \vdots & \ddots & \vdots & \vdots & \vdots & \vdots & \ddots & \vdots \\ \neq 0 & \cdots & \neq 0 & 0 & 0 & 0 & \cdots & 0 \end{bmatrix} \tag{5.10}$$

The five distinct individual matrices/vectors that can be made out are:

1. A square zero matrix of order $n_g - 1$.
2. A column vector of elements with negative unity, order $n_g - 1$.
3. Identity matrix of order $n_g - 1$.
4. Function matrix of order $n_g \prod n_g - 1$.

5. A square zero matrix of order n_g.

These five divisions can be utilized to simplify the mathematical construct that is used in the applications elucidated later in this section.

$$A = \begin{bmatrix} Z_{(n_g-1)\prod(n_g-1)} & -U_{n_g-1} & I_{n_g-1} \\ F_{n_g\prod(n_g-1)} & & Z_{n_g\prod n_g} \end{bmatrix} \tag{5.11}$$

Define $A_\lambda = \lambda I - A$ for some scalar quantity λ. Thus, the structure of A_lambda obtained is:

$$A_\lambda = \begin{bmatrix} \lambda I_{(n_g-1)} & -U_{n_g-1} & I_{n_g-1} \\ F_{n_g\prod(n_g-1)} & & \lambda I_{n_g} \end{bmatrix} \tag{5.12}$$

For the system to have transients indicative of frequency instability, there should exist some λ such that its real part is positive, that is:

$$\exists\, \lambda' \in Sol\{|A_\lambda| = 0\} : Re\{\lambda'\} \;>\; 0$$

Thus, the goal of the mathematical construct that is desired to be obtained is to make it indicative of some λ' such that it can be utilized to provide greater information about the system parameters. Thus, define a matrix the same order of A_λ, called a "Spoof" matrix, with all elements except those corresponding to the position of $F_{n_g\prod(n_g-1)}$ as zero. Let the matrix be denoted as ΔF with the elements being denoted as $\Delta f_i j$.

Let ΔF_i be a matrix that denotes each column of ΔF matrix that has at least one nonzero element. For some column vector u_i which has zeros in all elements except the i$^{\text{th}}$ element corresponding to +1, ΔF_i. Now, define $\Delta F_i'$ as $\Delta F_i \prod u_i$. Thus,

$$\Delta F = \Delta F_1' + \Delta F_2' + \cdots + \Delta F_{n_g-1}' \tag{5.13}$$

Thus, the desired matrix that is indicative of a point of instability can be obtained as

the sum of a few column vectors multiplied by a single element. Alternatively, they can be obtained (possibly faster) by merely appending $n_g - 1$ number of column vectors, but, the multiplicative notation is used as it allows for greater simplification in the final mathematical construct.

By Matrix determinant lemma, for a square matrix X, column vectors y and z, the determinant of their sum $X + yz^T$ can be expressed as:

$$|X + yz^T| = |X|(1 + z^T X^{-1} y) \tag{5.14}$$

Thus, the determinant of the desired state transmission matrix $A_\lambda^{'}$ that is indicative of system instabilities can be computed as:

$$|A_\lambda^{'}| = |A_\lambda + \Delta F| = |A_\lambda + \Delta F_1^{'} + \Delta F_2^{'} + \cdots \Delta F_n^{'}| \tag{5.15}$$

This can be further simplified as:

$$|A_\lambda^{'}| = |\sum_{i=1}^{n_g - 1} \Delta F_i \cdot u_i| \tag{5.16}$$

However, the final matrix obtained is of one where the matrix determinant lemma has to be applied recursively. This is computation expensive. The recursive equation obtained is a nonlinear sum of a linear sum of linearized nonlinear equations. Further linearization need not necessarily be helpful in maintaining the accuracy of the system model. Small signal model in its fundamental premise neglects parameters like damping and makes assumptions about power input and rotor=voltage angle synchronization. Any further approximation will add to the errors.

However, for Power Systems, it was observed based on trial runs on various systems (Six systems with 2, 3, 4, 5, 7 and 54 generators) that using just the first summation term was sufficient to obtain an matrix that serves the same purpose as the one computed with the

recursive set of equations. That is, this complex equation can be simplified by considering only one of the ΔF_i matrices. While, sometimes (Always, for larger systems!), the same $A_\lambda^{'}$ will not be obtained, it is important to note that the goal is to get an $A_\lambda^{'}$ that does not violate a desired set of system constraints and is indicative of instability, not to find an $A_\lambda^{'}$using the most accurate difference equations. The mathematical construct is not the final result, but, an intermediary result that is used to compute the mismatch in each iteration that leads to the final results. Hence, simplifying the difference equations to compute it can be done without affecting the final results, it only increases the number of iterations required and the final parameter-wise distribution, not the nature of the results itself.

Thus, considering only the first column vector yields:

$$|A_\lambda^{'}| = |A_\lambda + \Delta F_1 \cdot u_1| = (1 + u_1^T A_\lambda^{-1} \Delta F_1)|A_\lambda| \tag{5.17}$$

Utilizing the cofactor matrix of A_λ, $co(A_\lambda)$ and further simplification yields:

$$|A_\lambda^{'}| = \left(1 + \frac{1}{|A_\lambda|}[1\,0\,0\,\cdots\,0] co(A_\lambda)^T \begin{bmatrix} 0 \\ \\ \Delta F_{1p} \end{bmatrix}\right)|A_\lambda| \tag{5.18}$$

After multiplying the above rows, columns and simplifying, the final equality constraint for instability obtained is:

$$\lim_{\lambda \to 0}(|A_\lambda| + \sum_{p=1}^{n} C_{(p+n-1,1)} \Delta F_{p,2}) = 0 \tag{5.19}$$

Where C is the cofactor matrix of A_λ and the indices p, n, and 2 indicate the generator number and not matrix row/columns.

Thus, using the above equation (Eqn. 5.3) as an equality constraint, various optimization problems can be deployed, which elucidated in the following sections. A more detailed, stepwise derivation of the equation is provided in the appendices, along with another simpler, but, computationally more expensive mathematical construct that is obtained along with it.

5.4 Application: Small Signal Stability Model Based Power System Spoof Attack

The above mathematical constraint acts as a powerful tool when a reasonably accurate estimate of the system states are known. One such applications of it include the generation of spoof attacks for a randomly selected number of parameters, or, a targeted set of parameters. The primary goal of a motivated attacker with access to system states would be to launch spoof attacks that forces the system to respond in an undesirable way. This could include extreme situation like spoofing parameters to make it seem that line currents are above normal levels. Since they are physically not so, they would not be picked up by local protection systems, leading to a wider area system response that leads to frequency instability that triggers other protection devoces, and possibly, investigation into the functioning of the local protection systems. While attacks generated with such techniques do not have the capability to cause major damage to operation, they do cause economic penalties. The goal can be said to be to use the small signal stability model of the system to find some spoof vector that can force a system from normal operation state to Alert/Emergency state (Converse is also possible). This is illustrated in Fig 5.3*.

The SSSV based spoof attack generator model operates in two stages, namely, (i) The Parameter Checker, and (ii) The Spoof Value Generator. The first stage requires an estimate of relevant system states to function. Based on the states available, either a set of random parameters that are observable based on the states, or, a target set of states desired by the user are selected. These parameters are computed using an iterative method such that Eqn. 5.3 is satisfied. Once this is obtained, the second stage computes the values of the parameters that satisfies the equation. The overall process is implemented using the following steps:

*The base image for which is reproduced from ECEN 615 (Fall 2018) Lecture note # 27 of T. Overbye (Dept of ECE, TAMU), which is derived from L.H. Fink and K. Carlsen, Operating under stress and strain, IEEE Spectrum, March 1978, pp. 48-53. [12]

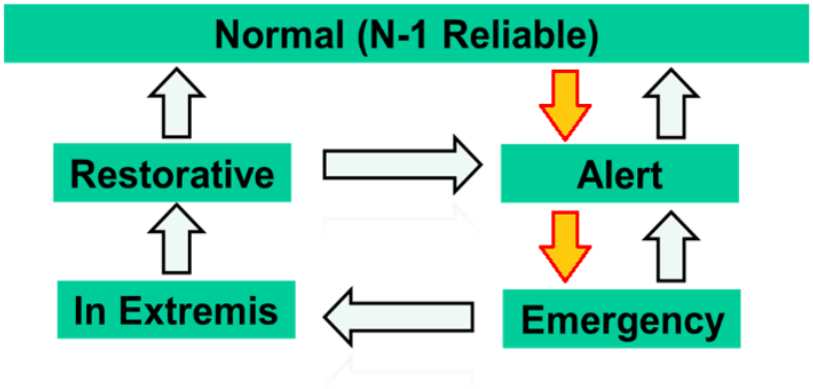

Figure 5.3: Objective of Utilizing the Small Signal Stability Vulnerability (SSSV) Model to generate Spoof Attacks. The direction of the goal is highlighted in orange.

1. Form a function matrix,

$$F_S^{'} = \begin{bmatrix} P_1 \\ P_2 \\ \vdots \\ P_n \\ Q_1 \\ Q_2 \\ \vdots \\ Q_{n-k} \\ V_{pv1} \\ \vdots \\ V_k \\ f_S \end{bmatrix} \tag{5.20}$$

   where f_S denotes Eqn. 5.3.

2. Compute the partial derivatives of the new function mismatch matrix, $F_S^{'}$ with respect to the selected parameters. Let this be the modified Jacobian Matrix, J_S.

3. Use iterative Newton-Raphson technique to solve for the parameters from their current

estimate to a value that forces all mismatch equations, including f_S to tend to zero.

4. Enforce any constraints necessary on the parameters and continue iterations till convergence.

5. Once convergence is obtained, the present values of the parameters are outputted as the final spoof values.

It should be noted that the recursive computations in the above techniques can be utilized with additional constraints such as line limits etc., but, since only a certain fraction of the measurements are utilized, unless the new states vary widely from the original, no line limits will be avoided. While implementing this algorithm in §5.4.3, constraints are placed on the spoofed variables so that they do not violate any operating limits, thereby ensuring that the values do not deviate greatly from their original value, and also passively enforcing line limits. Line limits can be additionally included in this algorithm, but, given that constraints on the parameters themselves can be constructed to account for constraints on limits, it can be excessive. While directly including the line limits would make it straightforward to compute the constraints on the parameters being spoofed, the addition of additional constraints increases convergence time. However, the common ground is that any reasonable constraint on system operation can be implemented. A more *tight* constraint, wherein, a parameter is not allowed to greatly vary is less likely to provide a set of parameters that can induce frequency instability unless the number of parameters chosen enough are large enough. These tradeoffs are discussed during the application of this method to the IEEE 118-Bus system.

The key characteristics of the mathematical construct are:

1. Since stability is checked as a loop condition, simplification of the matrix determinant condition is immaterial to the results.

2. Pseudoinverse always exists for a stable system with a normal N-R solution. Hence, iterations are not constrained.

3. Can be used to generate spoof attack values for all steady-state parameters:

   (a) Real Power (Generation and Load)

   (b) Reactive Power (Generation and Load)

   (c) Bus Voltages

   (d) Bus Angles

The overall process of generating spoof parameters is illustrated in Fig. 5.4. The application of the equation is explained with equations for a few smaller systems in the following subsections before its demonstration for a larger system.

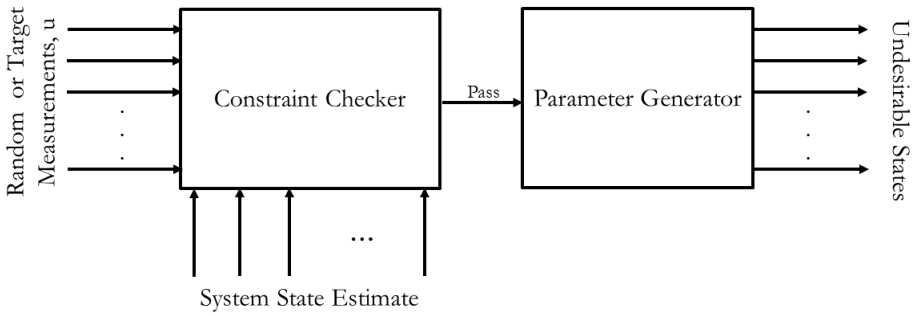

Figure 5.4: Stage-wise Depiction of the SSSV Spoof Attack Generator Model.

5.4.1 Application: 2 Generator System

Consider a system with 2 generators, and an equivalenced circuit as shown in Fig. 5.5. The equivalent Transmission matrix is:

$$A_\lambda = \begin{bmatrix} \lambda & -1 & 1 \\ F_{11} & \lambda & 0 \\ F_{12} & 0 & \lambda \end{bmatrix} \tag{5.21}$$

Solving the above matrix to find a λ that has a positive real part yields the constraint $F_{11} - F12 > 0$. Assuming that F_{11} and F_{12} are of the forms $-Acos\delta_{12}^* - Bsin\delta_{12}^*$ and $-Ccos\delta_{12}^* - Dsin\delta_{12}^*$ respectively (Using Eqn. 5.7), the constraint is simplified to:

$$tan\delta_{12}^* > \frac{C-A}{D-B}$$

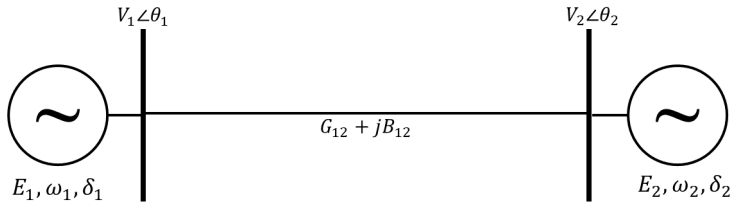

Figure 5.5: Equivalencing a system with 2 Generators into a 2-Bus Equivalent. Equivalent Loads not depicted.

Thus, for this elementary case, the values of A, B, C, D should be optimized to get the desired parameter values.

5.4.2 Application: 3 Generator System

In this case (Fig. 5.6), the presence of three generators in a system produces six function terms, labeled as F_{ij}, with the indices taking possible values of i = 1,2,3 and j = 1,2. Repeating the same process as in the 2 Generator case, the constraint obtained is

$$F_{11}(F_{22} - F_{32}) + F_{21}(F_{32} - F_{12}) + F_{31}(F_{12} - F_{22}) > 0$$

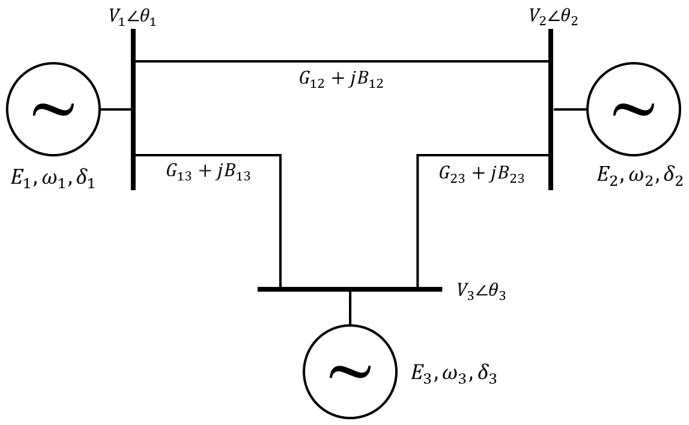

Figure 5.6: Equivalencing a system with 3 Generators into a 3-Bus Equivalent. Equivalent Loads not depicted.

Optimizing the selected parameters based on the above relation provides the desired spoof values. No simple pattern relating the parameters and stability boundaries exist for scenarios with more than three generators.

5.4.3 Application: IEEE 118-Bus System

The IEEE 118-Bus System (Same as the one used in previous sections) is used as a base to generate spoof attacks that cause frequency instability in the system. The parameters chosen for the attack generation were bus voltages and angles, although scope for inclusion of other system variables exist, as discussed previously.

While computing the voltages and angles, the voltages were restricted to $0.90 - 1.15$ p.u. while the angles were restricted to $0 \pm 27°$. If any of the original voltages or angles fell outside the angle, they were allowed to vary till that limit. The initial test was performed using a random number of evenly distributed selections, starting with a minimum of two measurements compromised, and progressing upto 40 measurements. Fig. 5.7 shows percentage of attacks that were successful in pushing the system from normal (N – 1 reliable) operation state to alert/emergency states based on the number of random buses selected for attacks. A total of 2000 random attacks were conducted, from which 157 were filtered in the first stage as effective. It is important to note that the barchart in Fig. 5.7 does not show probability of attack vector being undetected or probability of injection, but, probability of causing physical parameters of the system (System States) to respond undesirably given that an attack was successful.

It should be noted that while machine damping is ignored in the iterative computations, a simplified damping model, with a positive damping factor is assumed when checking for the stability and the success of the attack. It is worth noting that if damping is not considered all together, then, the success rate would consistently be 100%, and should the developed model work solely in such cases where damping is completely ignored, it would make it impossible to practically utilize it.

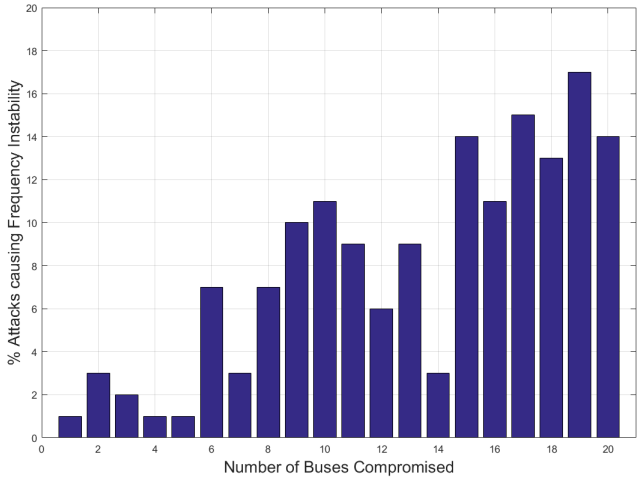

Figure 5.7: Initial Results of Evenly Distributed Random Attacks on the IEEE 118-Bus System.

Although an increase in probability of attack success is expected as number of target buses increase, this general trend has as many exceptions in the results as adherences in the result. This is most probably due to the number of random combinations used being smaller than the possible number of combinations. For instance, 100 random buses of 118 possible buses were tested for 1 bus attack scenario. However, when 2 bus scenarios was considered, only 100 of 6903 possible 2 bus attacks were tested. The greatest outlier from the ascending trend was when a combination of 14 random buses were used to attack the system. The code tested only 100 of the possible 5.21E17 combinations! Thus, another blind random test was executed, to compare the results. The results of this run are presented in Fig. 5.8.

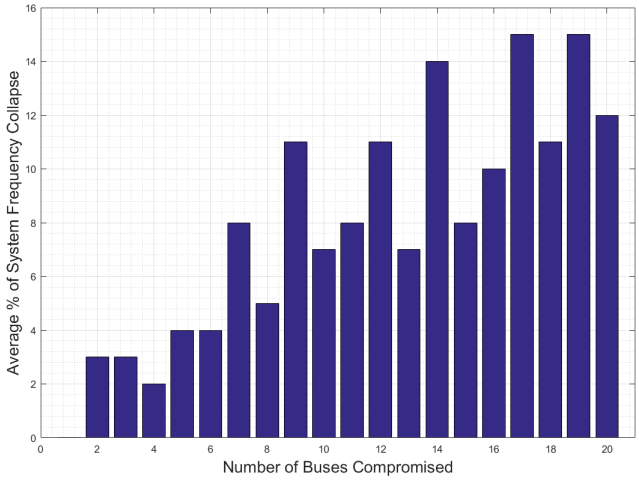

Figure 5.8: Results of Evenly Distributed Random Attacks on the IEEE 118-Bus System after Second Run.

Following this blind testing, the system was selected for a more systematic number of attacks. 100 unobservable attack vectors covering 20 measurements across the system were crafted, with the selection of measurements being random. While the randomness of selection is reduced (In the sense of randomness in number of measurements selected being selected), the measurements are targeted. This provides a significantly improved result, with a 12x (Twelve times) improvement in the success rate. At this junction, it is important to note that 'Success rate' is considered to be the probability of selected a set of measurements that can be used to launch an unobservable attack that causes frequency instability. Following this, the number of randomly attacked measurements is increased to 10% of the total number of voltage and angle measurements in the system. No improvements in the success rate was observed. For this scenario, the movement of the eigenvalues of the State Transmission Matrix for two of the one hundred scenarios is depicted in Figures 5.9 and 5.10.

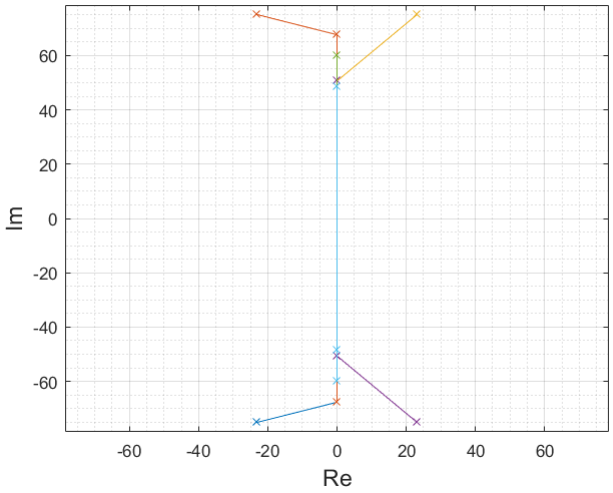

Figure 5.9: Movement of Eigenvalues of the Transmission Matrix (from LHS to RHS of the Re-Im plane) for a scenario where instability was induced after two iterations.

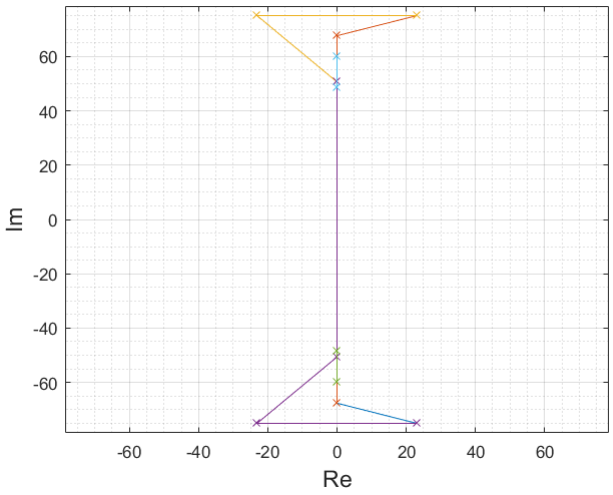

Figure 5.10: Movement of Eigenvalues of the Transmission Matrix (from LHS to RHS of the Re-Im plane) for a scenario where instability was induced after four iterations.

Following this, targeted attacks were launched at the system, with the targets being selected by decomposing the Vulnerability Equation, f_S into bus-wise terms. A wide ranging

number of attacks, starting at 10 buses/20 measurements and going upwards of 40 measurements were employed. This provided a significantly much larger success rate.

The results of all the above scenarios are tabulated in Table 5.2.

Table 5.2: Summary of the various SSSV Model based Attacks on the IEEE 118-Bus System.

Method of crafting Attack Vector	Success Rate
Random (Number of measurements targeted unaccounted for)	0.75%
Random (10 buses targeted)	9%
Random (12 buses– 10% of total buses targeted)	9%
Random (Maximum success rate/No. of buses targeted)	16%/19 buses
Targeted (Overall)	33%
Targeted (Most efficient/No. of buses targeted)	60%/14 buses

5.5 Application: Defending Attacks launched using it

This section illustrates the applications of the SSSV model that can be used as defensive techniques that assist in system analysis. For defensive applications, the equality constraint is converted to an inequality constraint and the system is optimized for desirable results. This can be utilized as a method to improve system robustness.

$$\lim_{\lambda \to 0}(|A_\lambda| + \sum_{p=1}^{n} C_(p+n-1,1)\Delta F_{p,2}) \neq 0 \tag{5.22}$$

5.6 Further Applications: Conceptual Explanations

This section continues on the defensive applications of the SSSV model, but, provides only conceptual explanations, without providing for numeric results. Some of the results are similar to those presented in earlier sections, while some others are beyond the scope of this work, and are hence, not elucidated further than their conceptual applications.

5.6.1 Recomputing Device Settings

This technique acts as a more powerful version of the DFM algorithm that is used to compute the settings of FACTs device. Unlike the DFM algorithm that required conversion of reactive power injection into apparent change in impedance, the SSSV model is more directly, allowing for direct injections of reactive power to be incorporated in it. It can be compliment with models of the FACTs device to get the settings of the device directly, so as long as the model can be used to obtain a partial differential (sensitivity) equation that is reflective of the device's range of operation states.

While the SSSV Model is far more powerful, it is more complicated, taking longer time to perform similar computations. For D-FACTs devices, as previously demonstrated using DFM algorithm, the SSSV model can be used to compute apparent change in impedance. For traditional FACTs devices computed to buses, it can be used to computed reactive injection. Since the numeric results corresponding to this application are same as those presented in the previous section, they are not repeated here.

5.6.2 Analyzing Impact of Data Accuracy on System Responses

The analysis of change in system parameter values on its response using the SSSV model is obtained by including the parameter as a variable to be spoofed. In this scenario, instead of acceptable range of parameters being based on operating characteristics, the % uncertainty in the measurement is used to set the acceptable range of the parameter(s). Once this is set, the mathematical construct is iteratively computed, with the final steady state results (That correspond to highest level of uncertainty of the combination) being indicative of system response during worst-case response. It is important to note that the worst-case uncertainty of the set of parameters need not correspond to the individual worst-case uncertainties, as a system is linear. That is, for instance, if a set of parameters include a load estimate of 150

MW ± 10%, then, it is possible that the overall worst case points to an uncertainty that is neither +10%, nor -10% of the load estimate.

6. SUMMARY

In this thesis, the first section presented a review of literature relevant to the work presented in the later sections. The first original work presented in this thesis, namely, the use of Bayesian Networks of system clustering analysis provided an insight into alternative avenues to analytic computation techniques for clustering analysis of FACTs devices, and, power-system lines in general.

The following section introduced the Distributed Failure Mitigation (DFM) Algorithm that provides an iterative computation technique to compute the settings of controllers to meet a specified adjective. The same section indicates the use of existing literature to the thesis, demonstrating the use of existing techniques and combining it with the DFM algorithm to provide an overall system response to tackle device failure and coordinated attacks.

The next section provided insights into techniques of analyzing system vulnerability and using a common mathematical construct to both study offensive and defensive strategies towards system operation. The offensive operations were demonstrated with the use of generating spoof voltage values to force the system to shift from normal (N - 1 Reliable) operating state to an alert state. The defensive operations were conceptually explained to indicate how to avoid vulnerability points in the system operating states. It additionally explained the usage of the mathematical construct to compute controller settings.

The first section of original work explored alternative methods to fasten dynamic device selection while the second provided analytic techniques of response. The final section provided a larger perspective on vulnerabilities of system to frequency instability and undesired triggering of local protection systems, with indications of how it can be constructed to incorporate the strategies presented in the first two sections of initial work.

7. CONCLUSION

7.1 Conclusion

This thesis introduced the use of probabilistic graphical models for dynamic reactive support device selection, methodologies of computing controller settings on-line and a broader technique of analyzing system vulnerabilities. The computation techniques were deployed for D-FACTs, which are practically deployed and allow for dynamic change in settings. Thus, apart from primarily mitigation of device failures and misoperations, the algorithms can be used to fine-tune the system response to improve economic operation, which can be achieved by using an appropriate control objective. The vulnerability analysis provides insights into the interactions of the various parameters in the system and highlights how certain combination of parameters that result in stable steady-state operation can have transient responses that deviate considerably from an ideal response.

In summary, contribution of this thesis to existing literature is:

1. Usage of Graphical Models to explore scope of improving controller operation.

2. Developing analytic techniques of computing controller techniques that can be used in situations of failure, misoperation, or, be used to fine-tune controller settings to meet a control objective.

3. Provide insights into system operation by indicating what desired steady-state states of operation are achieved through non-stable or non-optimum transient paths of system frequency.

7.2 Potential for Future Work

The potential for future work includes the incorporation of more system parameters to improve the predictions of the Bayesian Network based inference technique, apart from utilizing multinomial states. The techniques of vulnerability analysis can be extended to

compute controller operation states. The present technique uses the fundamental Small Systems Stability model, and usage of more accurate and detailed models developed since will provide far better results and more accurate insights.

REFERENCES

[1] C. C. Liu, A. Stefanov, J. Hong, and P. Panciatici, "Intruders in the grid," *IEEE Power and Energy Magazine*, vol. 10, no. 1, pp. 58–66, Jan 2012.

[2] N. Falliere, L. O. Murchu, and E. Chien, "W32.Stuxnet dossier," Symantic Security Response, Tech. Rep., Oct. 2010.

[3] J. Valenzuela, J. Wang, and N. Bissinger, "Real-time intrusion detection in power system operations," *IEEE Transactions on Power Systems*, vol. 28, no. 2, pp. 1052–1062, May 2013.

[4] R. B. Bobba, K. M. Rogers, Q. Wang, H. Khurana, K. Nahrstedt, and T. J. Overbye, "Detecting false data injection attacks on dc state estimation," *Workshop on Secure Control Systems (SCS), Stokholm*, 2010.

[5] G. Chaojun, P. Jirutitijaroen, and M. Motani, "Detecting false data injection attacks in ac state estimation," *IEEE Transactions on Smart Grid*, vol. 6, no. 5, pp. 2476–2483, Sept 2015.

[6] S. Hossain-McKenzie, M. Kazerooni, K. Davis, S. Etigowni, and S. Zonouz, "Analytic corrective control selection for online remedial action scheme design in a cyber adversarial environment," *IET Cyber-Physical Systems: Theory & Applications*, 2017.

[7] Control Systems Security Program (CSSP), DHS, "Department of Homeland Security Control Systems Security Program," 2007. [Online]. Available: http://s3.documentcloud.org/documents/1212530/14f00304-documents.pdf

[8] B. Wayne Bequette, *Process Control: Modeling, Design, and Simulation*. Prentice Hall PTR, 2003.

[9] K. M. Rogers and T. J. Overbye, "Some applications of distributed flexible ac transmission system (d-facts) devices in power systems," in *2008 40th North American Power*

Symposium, Sept 2008, pp. 1–8.

[10] K. Rogers, "Power system control with distributed flexible ac transmission system devices," Master's thesis, University of Illinois at Urbana-Champaign, 2009.

[11] A. Hamdan and A. Elabdalla, "Geometric measures of modal controllability and observability of power system models," *Electric Power Systems Research*, vol. 15, no. 2, pp. 147 – 155, 1988.

[12] L. Fink and K. Carlsen, "Operating under stress and strain," *IEEE Spectrum; (United States)*, Mar 1978.

[13] D. Kundur, *Lecture notes in ECEN 689: Cyber Security of the Smart Grid*. Texas A & M University, 2011. [Online]. Available: https://www.comm.utoronto.ca/~dkundur/course_info/smart-grid-sec/presentations/KundurFalseDataInjAttacks_handouts.pdf

[14] G. Peters and J. H. Wilkinson, "The least squares problem and pseudo-inverses," *The Computer Journal*, vol. 13, no. 3, pp. 309–316, 1970.

[15] J. Chen and A. Abur, "Placement of PMUs to enable bad data detection in state estimation," *Power Systems, IEEE Transactions on*, vol. 21, no. 4, pp. 1608–1615, Nov. 2006.

[16] S. Hossain-McKenzie, K. Davis, M. Kazerooni, S. Etigowni, and S. Zonouz, "Distributed controller role and interaction discovery," in *2017 19th International Conference on Intelligent System Application to Power Systems (ISAP)*, Sept 2017, pp. 1–6.

[17] S. Hossain-McKenzie, K. Raghunath, M. Kazerooni, K. Davis, S. Etigowni, and S. Zonouz, "Sdcd: A strategy for distributed controller defense in cyber-adversarial power systems," in *Under Review*.

[18] D. C. Yu, T. C. Nguyen, and P. Haddawy, "Bayesian network model for reliability assessment of power systems," *IEEE Transactions on Power Systems*, vol. 14, no. 2, pp. 426–432, May 1999.

[19] Y. Hu, A. Kuh, T. Yang, and A. Kavcic, "A belief propagation based power distribution system state estimator," *IEEE Computational Intelligence Magazine*, vol. 6, no. 3, pp. 36–46, Aug 2011.

[20] R. Singh, E. Manitsas, B. C. Pal, and G. Strbac, "A recursive bayesian approach for identification of network configuration changes in distribution system state estimation," *IEEE Transactions on Power Systems*, vol. 25, no. 3, pp. 1329–1336, Aug 2010.

[21] Z. Yongli, H. Limin, and L. Jinling, "Bayesian networks-based approach for power systems fault diagnosis," *IEEE Transactions on Power Delivery*, vol. 21, no. 2, pp. 634–639, April 2006.

[22] D. Koller, N. Friedman, and F. Bach, *Probabilistic Graphical Models: Principles and Techniques*, ser. Adaptive computation and machine learning. MIT Press, 2009.

[23] B.-J. Yoon, "Texas A&M University; ECEN 689:602 Advanced PGM. Lecture on Jan 30, 2018."

[24] ——, "Texas A&M University; ECEN 689:602 Advanced PGM. Lecture on Feb 13, 2018."

[25] ——, "Texas A&M University; ECEN 689:602 Advanced PGM. Lecture on Mar 29, 2018."

[26] PowerWorld Corporation. (2016) D-FACTS Quick-Start Tutorial. http://www.powerworld.com/knowledge-base/d-facts-quick-start-tutorial.

[27] S. Hossain-McKenzie, "Protecting the power grid: Strategies against distributed controller compromise," Ph.D. dissertation, University of Illinois at Urbana-Champaign, 2017.

[28] K. Rogers, R. Klump, H. Khurana, and T. Overbye, "Smart-grid -enabled load and distributed generation as a reactive resource," in *Innovative Smart Grid Technologies (ISGT), 2010*, Jan. 2010, pp. 1–8.

[29] K. Raghunath and K. Davis, "Mitigation of distributed controller failure," in *Clemson Power Conference*. IEEE, 2018.

[30] P. Pérez, P. Albertos, A. Sala, and S. Antonio, *Multivariable Control Systems: An Engineering Approach*, ser. Advanced Textbooks in Control and Signal Processing. Springer, 2004.

[31] R. Dorf and R. Bishop, *Modern Control Systems*. Pearson, 2016.

[32] M. Hong and C.-C. Liu, "Complete controllability of power system dynamics," in *Circuits and Systems, 2000. Proceedings. ISCAS 2000 Geneva. The 2000 IEEE International Symposium on*, vol. 4, 2000, pp. 241–244.

[33] P. Sauer, J. Chow, and M. Pai, *Power System Dynamics and Stability: With Synchrophasor Measurement and Power System Toolbox*. IEEE Press, 2017.

[34] O. H. Abdalla, S. A. Hassan, and N. T. Tweig, "Coordinated stabilization of a multimachine power system," *IEEE Transactions on Power Apparatus and Systems*, vol. PAS-103, no. 3, pp. 483–494, March 1984.

[35] R. Cowell, P. Dawid, S. Lauritzen, and D. Spiegelhalter, *Probabilistic Networks and Expert Systems: Exact Computational Methods for Bayesian Networks*, ser. Information Science and Statistics. Springer New York, 2006.

[36] F. Jensen, *Bayesian Networks and Decision Graphs*, ser. Statistics for engineering and information science. Springer, 2001. [Online]. Available: https://books.google.com/books?id=eu3zjgEACAAJ

[37] B. Xu and A. Abur, "Observability analysis and measurement placement for systems with pmus," in *Power Systems Conference and Exposition, 2004. IEEE PES*, vol. 2, Oct. 2004, pp. 943–946.

[38] D. M. Divan, W. E. Brumsickle, R. S. Schneider, B. Kranz, R. W. Gascoigne, D. T. Bradshaw, M. R. Ingram, and I. S. Grant, "A distributed static series compensator sys-

tem for realizing active power flow control on existing power lines," *IEEE Transactions on Power Delivery*, vol. 22, no. 1, pp. 642–649, Jan. 2007.

[39] H. Johal and D. Divan, "Design considerations for series-connected distributed FACTS converters," *IEEE Transactions on Industry Applications*, vol. 43, no. 6, pp. 1609–1618, Nov. 2007.

[40] B. Chen, K. Butler-Purry, and D. Kundur, "Impact analysis of transient stability due to cyber attack on facts devices," in *North American Power Symposium (NAPS), 2013*, Sept. 2013, pp. 1–6.

[41] Y. Xiang, Y. Zhang, L. Wang, and W. Sun, "Impact of UPFC on power system reliability considering its cyber vulnerability," in *T & D Conference and Exposition, 2014 IEEE PES*, April 2014, pp. 1–5.

[42] H. Gawand, A. Bhattacharjee, and K. Roy, "Control aware techniques for protection of industrial control system," in *India Conference (INDICON), 2014 Annual IEEE*, Dec. 2014, pp. 1–6.

[43] H. C. Leung and T. S. Chung, "Optimal placement of FACTS controller in power system by a genetic-based algorithm," in *Power Electronics and Drive Systems, 1999. Proceedings of the IEEE 1999 International Conference on*, vol. 2, 1999, pp. 833–836.

[44] "Report on the grid disturbances on 30th july and 31st july 2012," Government of India, Tech. Rep., 2012. [Online]. Available: http://www.cercind.gov.in/2012/orders/Final_Report_Grid_Disturbance.pdf

[45] K. Bhattacharya, M. Bollen, and J. Daalder, *Operation of Restructured Power Systems*, ser. Power Electronics and Power Systems. Springer US, 2001.

[46] M. Correa, C. Bielza, and J. Pamies-Teixeira, "Comparison of bayesian networks and artificial neural networks for quality detection in a machining process," *Expert Systems with Applications*, vol. 36, no. 3, Part 2, pp. 7270 – 7279, 2009. [Online]. Available: http://www.sciencedirect.com/science/article/pii/S0957417408006593

[47] T. Liacco, "The adaptive reliability control system," *IEEE Transactions on Power Apparatus and Systems*, vol. PAS-86, no. 5, pp. 517–531, May 1967.

[48] D. M. Divan, W. E. Brumsickle, R. S. Schneider, B. Kranz, R. W. Gascoigne, D. T. Bradshaw, M. R. Ingram, and I. S. Grant, "A distributed static series compensator system for realizing active power flow control on existing power lines," *IEEE Transactions on Power Delivery*, vol. 22, no. 1, pp. 642–649, Jan. 2007.

[49] B. Xu and A. Abur, "Observability analysis and measurement placement for systems with pmus," in *Power Systems Conference and Exposition, 2004. IEEE PES*, vol. 2, Oct. 2004, pp. 943–946.

[50] H. Johal and D. Divan, "Design considerations for series-connected distributed FACTS converters," *IEEE Transactions on Industry Applications*, vol. 43, no. 6, pp. 1609–1618, Nov. 2007.

[51] S. Zonouz, K. Rogers, R. Berthier, R. Bobba, W. Sanders, and T. Overbye, "SCPSE: Security-oriented cyber-physical state estimation for power grid critical infrastructures," *Smart Grid, IEEE Transactions on*, vol. 3, no. 4, pp. 1790–1799, Dec 2012.

[52] B. Chen, K. Butler-Purry, and D. Kundur, "Impact analysis of transient stability due to cyber attack on facts devices," in *North American Power Symposium (NAPS), 2013*, Sept. 2013, pp. 1–6.

[53] M. Vrakopoulou, P. M. Esfahani, K. Margellos, J. Lygeros, and G. Andersson, "Cyber-attacks in the automatic generation control," in *Cyber Physical Systems Approach to Smart Electric Power Grid*. Springer, 2015, pp. 303–328.

APPENDIX A

PROBABILITY TABLES FOR BAYESIAN NETWORK

This appendix provides a tabulation of the the probabilities of a node assuming a value of unity given the states of its parents. The results correspond to §3.4.

Table A.1: Probability Table of $P_{G1} = 1$.

P_2	P_3	$\mathrm{P}(P_{G1} = 1 \mid P_2, P_3)$
0	0	0.3295
0	1	0.470
1	0	0.470
1	1	0.6705

Table A.2: Probability Table of $P_{G2} = 1$.

P_2	P_4	$\mathrm{P}(P_{G2} = 1 \mid P_2, P_4)$
0	0	0.166
0	1	0.349
1	0	0.395
1	1	0.832

Table A.3: Probability Table of $P_{G4} = 1$.

P_3	P_4	P_5	P($P_{G4} = 1 \mid P_3, P_4, P_5$)
0	0	0	0.168
0	0	1	0.283
0	1	0	0.300
0	1	1	0.505
1	0	0	0.276
1	0	1	0.466
1	1	0	0.492
1	1	1	0.830

Table A.4: Probability Table of $I_1 = 1$.

P_{G1}	P($I_1 = 1 \mid P_{G1}$)
0	0.459
1	0.541

Table A.5: Probability Table of $I_2 = 1$.

P_{G1}	P_{G2}	P_{G5}	P($I_2 = 1 \mid P_{G1}, P_{G2}, P_{G5}$)
0	0	0	0.314
0	0	1	0.403
0	1	0	0.421
0	1	1	0.540
1	0	0	0.398
1	0	1	0.510
1	1	0	0.534
1	1	1	0.684

Table A.6: Probability Table of $I_3 = 1$.

P_{G1}	P_{G2}	P_{G5}	P($I_3 = 1 \mid P_{G1}, P_{G2}, P_{G5}$)
0	0	0	0.255
0	0	1	0.340
0	1	0	0.448
0	1	1	0.596
1	0	0	0.310
1	0	1	0.413
1	1	0	0.543
1	1	1	0.724

Table A.7: Probability Table of $B_1 = 1$.

I_1	P_{G1}	I_2	P($B_1 = 1 \mid I1, P_{G1}, I_2$)
0	0	0	0.4658
0	0	1	0.339
0	1	0	0.339
0	1	1	0.247
1	0	0	0.747
1	0	1	0.545
1	1	0	0.545
1	1	1	0.397

Table A.8: Probability Table of $B_2 = 1$.

P_{G1}	I_2	P($B_2 = 1 \mid P_{G1}, I_2$)
0	0	0.623
0	1	0.731
1	0	0.180
1	1	0.211

Table A.9: Probability Table of $B_3 = 1$.

I_3	P($B_3 = 1 \mid I_1$)
0	0.49505
1	0.5705

APPENDIX B

DERIVATION OF SSSV EQUATIONS

Step-wise derivation of the SSSV Model equation (Eqn. 5.3) is presented here.

Consider a generic 'n' generator system (Note: Notation change in the appendix from n_g to n).

$$|A_\lambda| \to 0 = \lambda C_{11} + (-1)^{n+1} C_{1n} + (-1)^{n+1} C_{1,n+1} \to 0 \tag{B.1}$$

Dividing the above equation by λ, resulting in a corresponding reduction of the order of C_{1n} and $C_{1,n+1}$ to C'_{1n} and $C'_{1,n+1}$ yields:

$$C_{11} + (-1)^{n+1} C'_{1n} + (-1)^{n+1} C'_{1,n+1} \to 0 \tag{B.2}$$

Dropping the row denotation in the cofactors, and accounting for the possible values of 'n' (that is, even and odd), yields the following constraint:

$$|C_1| - |C'_n - C'_{n+1}| = 0 \tag{B.3}$$

The above straightforward constraint can be utilized in lieu of Eqn. 5.3, but, it is not scalable for large systems. Hence, it is not implemented. Thus, going back to the representation of $A'_\lambda = A_\lambda + \Delta F$, and considering only one column of computations, the equation obtained is:

$$|A_\lambda + \Delta D_1 u_1^T| \to 0 = |A_\lambda|(1 + u_1^T A_\lambda^{-1} \Delta F_1) \to 0 \tag{B.4}$$

$$\implies |A_\lambda|(1 + \frac{u_1^T co(A_\lambda)^T \Delta F_1}{|A_\lambda|}) \to 0 \tag{B.5}$$

$$\implies u_1^T co(A_\lambda)^T \Delta F_1 + |A_\lambda| \to 0 \tag{B.6}$$

$$\implies [C_{11}\, C_{21}\, \cdots C_{n-1,1}\, C_{1,n}\, \cdots\, C_{1,2n-1}][0 \cdots 0 \Delta F_{11} \cdots \Delta F_1 n]^T + |A_\lambda| \to 0 \tag{B.7}$$

Simplifying the above equation yields,

$$\lim_{\lambda \to 0}(|A_\lambda| + \sum_{p=1}^{n} C_(p+n-1,1)\Delta F_{p,2}) = 0 \tag{B.8}$$